

# Techno-Economic Analysis of the hydrogen-based microgrid in the residential area

宮崎, 大河  
九州大学総合理工学府環境エネルギー工学専攻

<https://hdl.handle.net/2324/4785156>

---

出版情報 : 九州大学, 2021, 修士, 修士  
バージョン :  
権利関係 :

---

# Techno-Economic Analysis of the hydrogen-based microgrid in the residential area

---

**Taiga Miyazaki**

Supervisor

**Associate Professor. Hooman Farzaneh**



**February 2024**

Energy and Environmental System Laboratory,  
Department of Energy and Environmental Engineering  
Interdisciplinary Graduate School of Engineering  
Sciences

**KYUSHU UNIVERSITY**  
**Japan**

<b>ABSTRACT</b> .....	3
<b>CHAPTER 1: INTRODUCTION</b> .....	4
<b>1.1. BACKGROUND AND MOTIVATION FOR THIS STUDY</b> .....	4
<b>1.2. WHAT WILL BE ELUCIDATED IN THIS RESEARCH</b> .....	6
<b>CHAPTER 2: SIMULATION MODEL OF THE HRES COMPONENTS</b> .....	7
<b>2.1. BASIC CONCEPT OF THE PHOTOVOLTAIC (PV) SYSTEM</b> .....	7
<b>2.2. BASIC CONCEPT OF THE SOLAR ELECTROLYZER</b> .....	14
<b>2.3. BASIC CONCEPT OF THE FUEL CELL MODEL</b> .....	17
<b>2.4. MODEL VALIDATION WITH THE EXPERIMENTAL DATA</b> .....	21
<b>2.4.1. PV MODEL TEST</b> .....	21
<b>2.4.2. ELECTROLYZER</b> .....	23
<b>2.4.3. FUEL CELL</b> .....	25
<b>CHAPTER 3: DETAILED DESIGN OF THE HRES</b> .....	30
<b>3.1. HRES CONTROL STRATEGY</b> .....	30
<b>3.2. DEMAND LOAD PROFILE</b> .....	32
<b>3.3. SOLAR INCIDENT ON THE TILTED PV SURFACE</b> .....	33
<b>3.4. HRES SIZE ESTIMATION</b> .....	34
<b>CHAPTER 4: RESULTS AND DISCUSSION</b> .....	39
<b>CHAPTER 5: CONCLUSION</b> .....	47
<b>REFARENCE</b> .....	48

## Abstract

Nowadays, Japan faces two major problems. The first is the energy problem. Most of Japan's power generation is thermal power generation, which uses fossil fuel. And most of this fossil fuel is imported from abroad. For this reason, Japan's energy self-sufficiency rate is extremely low, and is said to be only about 9.6% [1]. Relying on imports of fossil fuels poses a major risk to the Japanese economy. Hence, raising the self-sufficiency rate of energy to mitigate these risks is an extremely important issue in Japan's security.

The second issue is global warming. Since the Industrial Revolution, humankind has rapidly developed civilization by using fossil fuels such as coal and crude oil, which are the main sources of carbon dioxide. Decarbonization using renewable energy is one of the methods that are attracting the most attention as a solution to global warming by generating electricity with renewable energy such as solar power generation and wind power generation instead of using fossil fuels to reduce carbon dioxide emissions. However, there is a big problem with the intermittency of the availability of renewable energy sources. "Hybrid Renewable Energy System (HRES)" is a solution to the above two problems. HRES is a method of generating electricity using multiple types of renewable energy, covering the weaknesses of each power generation method and achieving stable power generation.

In this study, we examined hydrogen-based HRES, which contains solar panels, solar electrolyzers and fuel cells. The solar panels generate more electricity during the day than the actual demand requirement, so the surplus electricity is used to generate hydrogen in the electrolytic device; the hydrogen is stored in the hydrogen storage, and fed to the fuel cell for generating electricity. A detailed simulation model is developed to estimate the hourly electricity and hydrogen generation from the proposed HRES. The size of the components is estimated, using the detailed electricity demand load in a typical Japanese house. The designed system is then applied to the residential area in Tokyo, Japan in order to evaluate the impact of the different weather conditions on the performance of the proposed HRES. The amount of power generation is simulated based on the weather data in 2020, and the "Levelized cost of energy (LCOE)" and "coverage rate" were calculated.

Keywords: Hybrid Renewable Energy System (HRES), Techno-Economic Analysis, Levelized Cost Of Energy (LCOE)

## Chapter 1: Introduction:

### 1.1. Background and motivation for this study

Global warming has become a problem these days. Fig. 1-1 shows the total world carbon emissions. Since the industrial revolution, carbon emission has increased significantly. If carbon emissions continue to increase, global warming will progress, and people will not be able to live on the earth. Therefore, it is necessary to reduce carbon emissions.

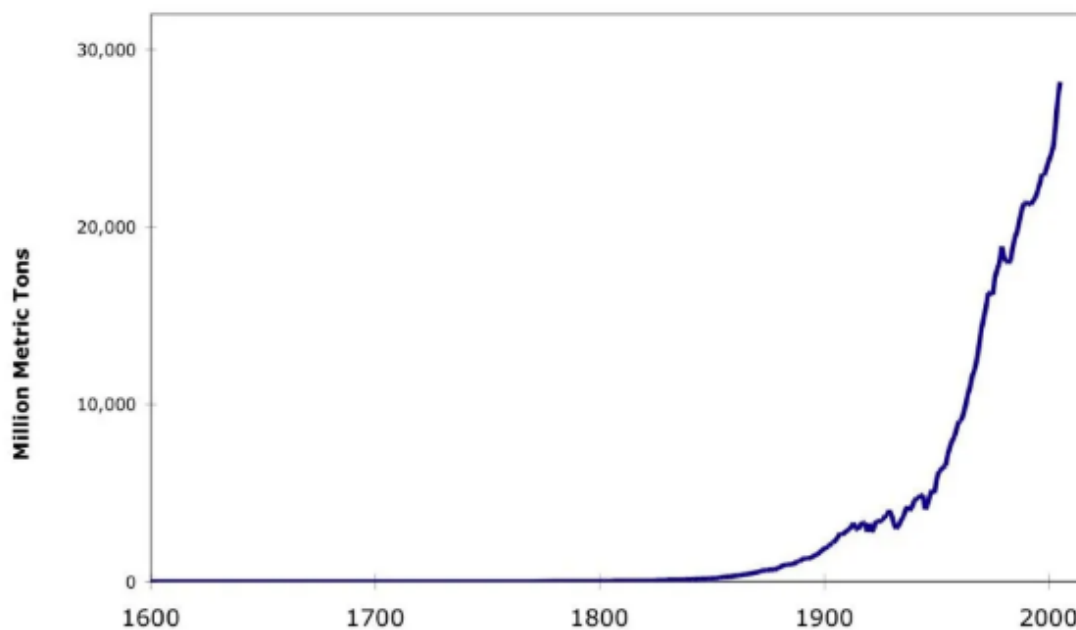


**Fig. 1-1 Total world carbon emission [1]**

The carbon emissions problem is a global problem and a concern in Japan. Fig. 1-2 shows Japan's energy self-sufficiency rate. Japan's energy self-sufficiency rate is about 9.6%. Japan imports about 90% of energy from overseas. The imported energy from overseas is basically fossil fuel. Renewable energy such as solar panels and wind power generation is expected to solve the global warming problem and the energy self-sufficiency rate.

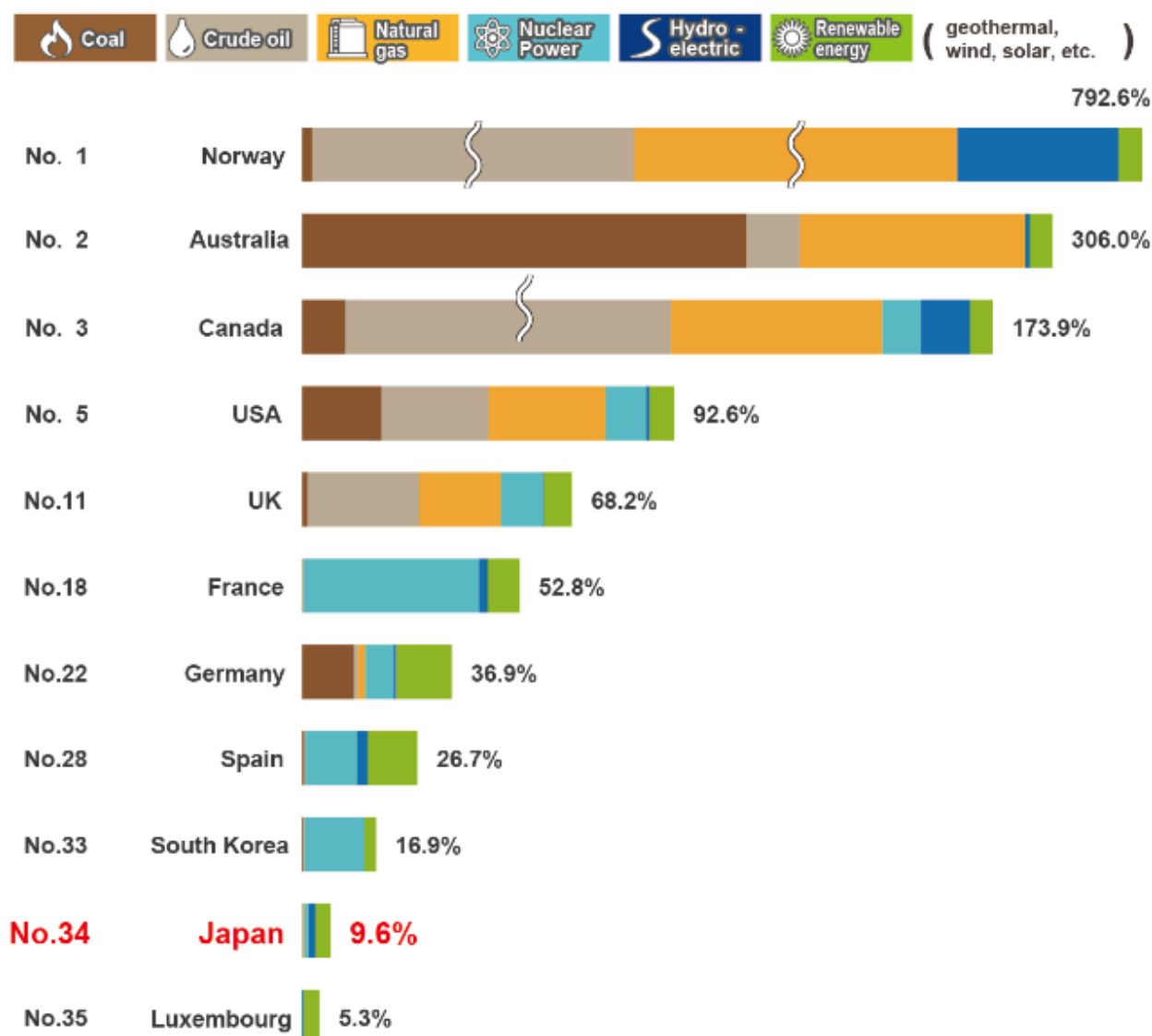


**Fig. 1-2 Energy self-sufficiency rate[2]**

Renewable energies such as solar energy do not emit carbon dioxide during power generation. However, renewable energy also has its weaknesses. Solar panels, for example, can only generate electricity while the sun is rising. Therefore, the Hybrid Renewable Energy System (HRES), which uses multiple resources and technologies to generate electricity, can be considered as the solution to tackle the intermittency problem of renewable energy sources.

## 1.2. What will be elucidated in this research

This study develops a simulation model of a “hydrogen-based Hybrid Renewable Energy System (HRES)”. Fig. 1-3 is the HRES flow chart produced in this research. This HRES uses PV- panels to generate electricity and supply it to the home residential building. And if the solar panel alone does not have enough power, it will be supplied provided from the grid. The surplus electricity supplied to the house is supplied to the electrolyzer to produce hydrogen. This hydrogen is stored in hydrogen storage. The hydrogen stored in the hydrogen storage is used in situations where the solar panel cannot generate enough electricity. Hydrogen in hydrogen storage is used in fuel cells to generate electricity when there is not enough electricity during the night. The HRES was applied to Tokyo in Japan to calculate “Levelized Cost Of Energy (LCOE)”.

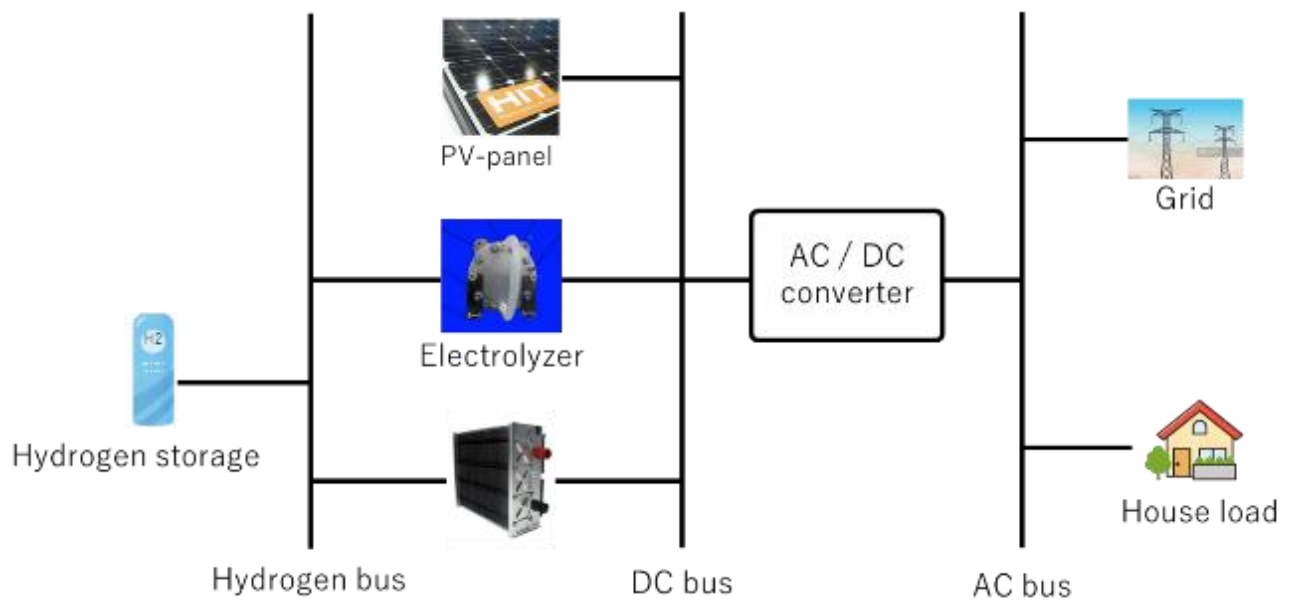


**Fig. 1-3 HRES flow chart**

## Chapter 2. Simulation Model of the HRES components:

### 2.1. Basic concept of the Photovoltaic (PV) system

PV panels are composed of multiple layers, as shown in Fig. 2-1. It consists of Electrode and Anti-Reflection Film, P-type semiconductor, N-type semiconductor.

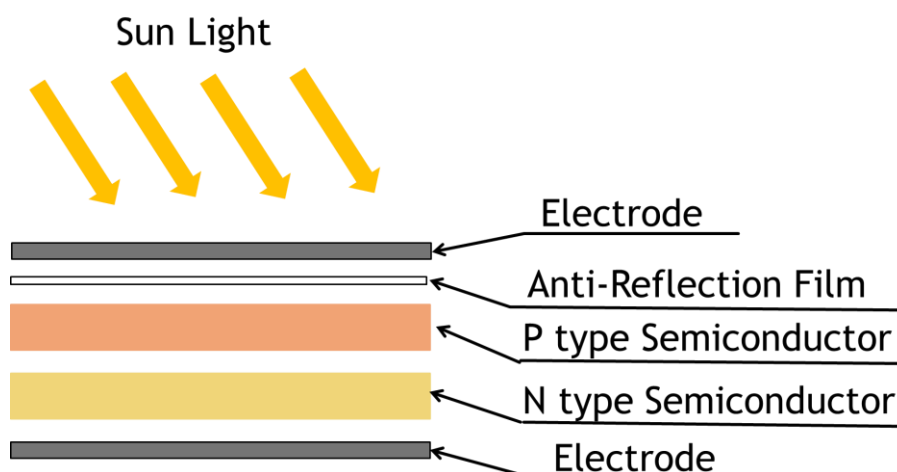


Fig. 2-1 PV-panel's overall structure [4]

P, N-type semiconductor's main component is silicon. But silicon only can't conduct electricity.

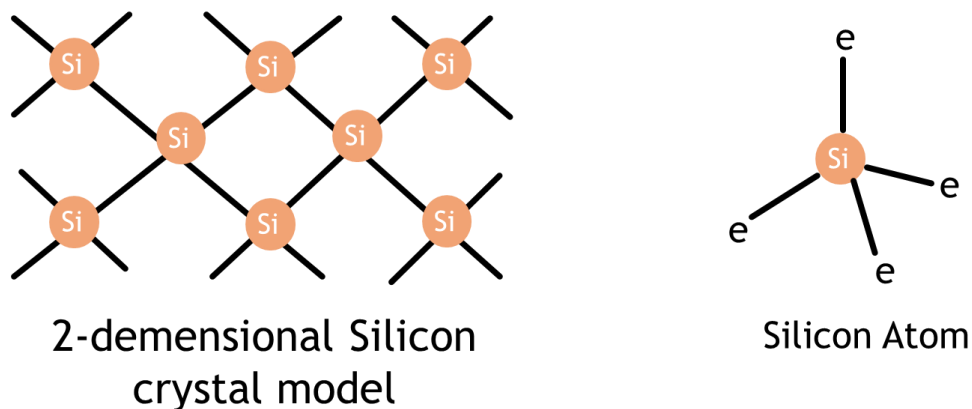


Fig. 2-2 Silicon structure [4]



So, adding phosphorus to silicon makes it a P-type semiconductor. This is called N-type dope. And N-type doping, the remaining free electrons can move freely.

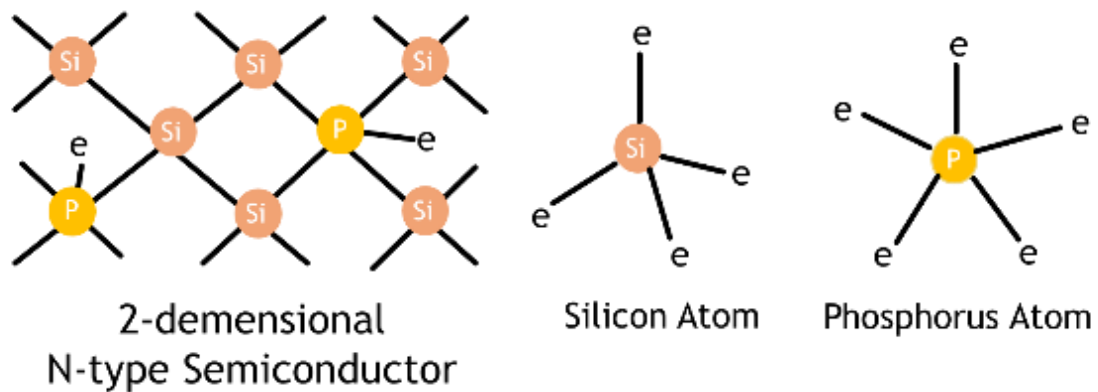


Fig. 2-3 N-type Semiconductor [4]

And adding Boron to silicon makes it a P-type semiconductor. This is called P-type dope. And P-type dope holes are generated because there are not enough electrons.

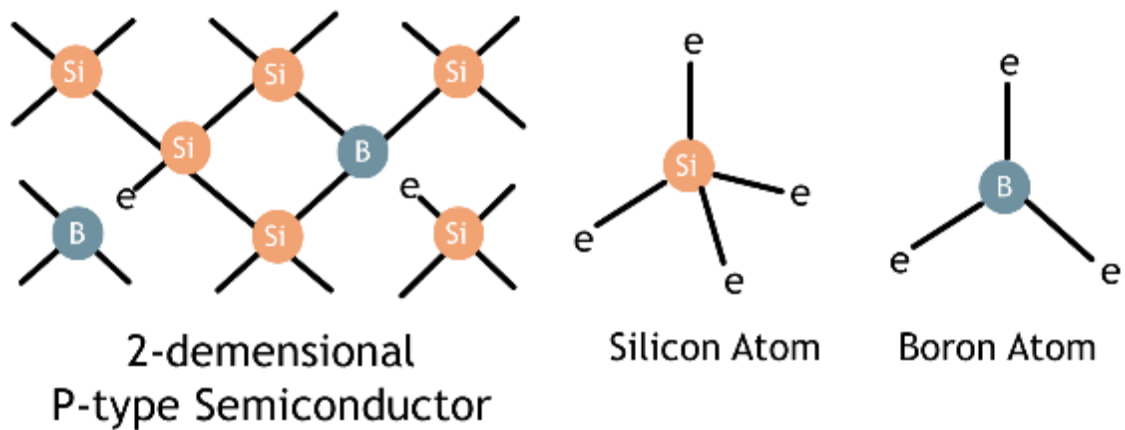


Fig. 2-4 P-type Semiconductor [4]

When a P-N junction is formed, a depletion layer is generated by moving free electrons to holes near the junction. As a result, the P-side is positively charged and the N-side is negatively charged.

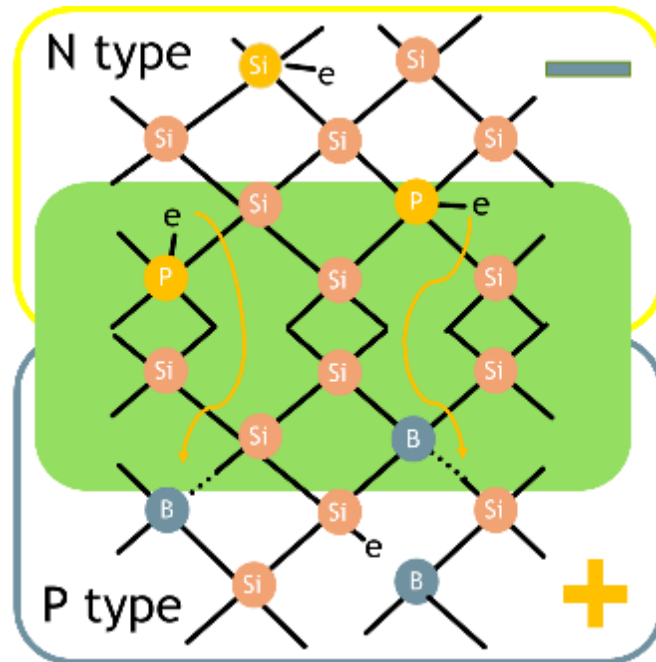


Fig. 2-5 PV-panel depletion layer [4]

When sunlight hits the depletion layer, it is separated into free electrons and holes in the depletion layer, free electrons move to the negative side, and holes move to the positive side. Then, the free electrons move. Through the lead wire to the negative electrode and combine with the holes. By repeating this, photovoltaic is working.

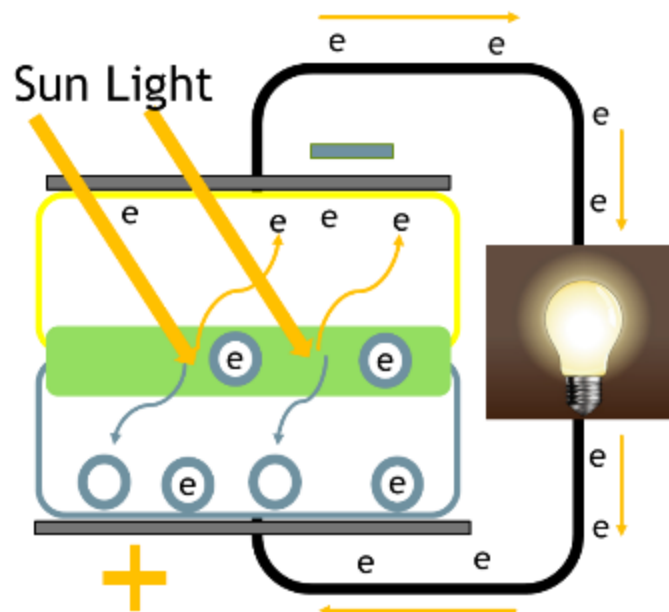
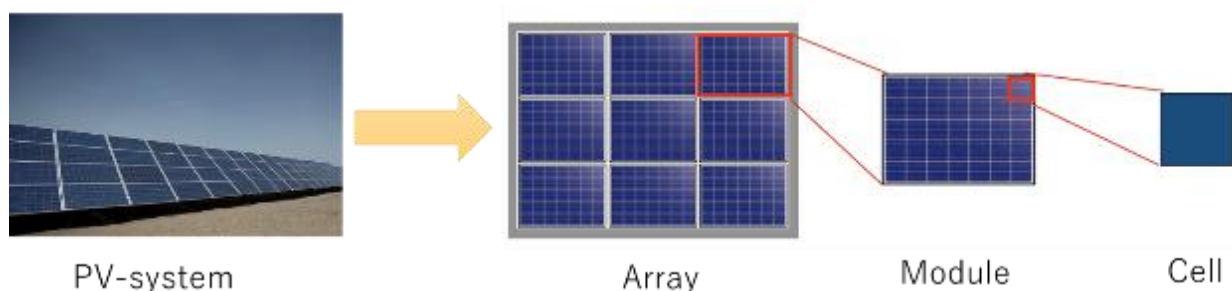


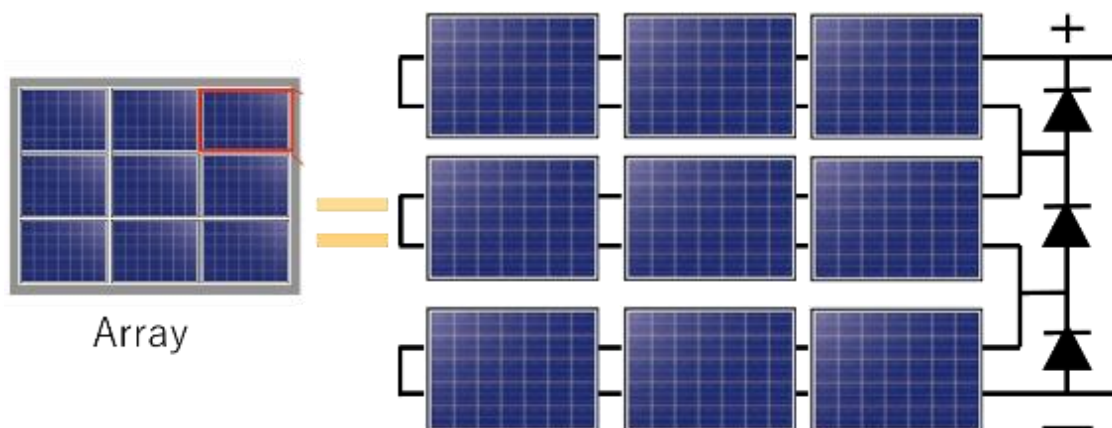
Fig. 2-6 PV-panel free electrons [4]

Fig. 2-7 shows the PV system structure. The PV system uses a huge collection of PV panels called arrays. An array consists of a collection of PV panels called modules. Then, if you divide the module further, you can divide it into small PV panels called cells.



**Fig. 2-7 Structure of PV systems [5]**

Diodes are connected in parallel to the modules that make up the PV array. This will include the diode in the equivalent circuit.



**Fig. 2-8 Diode parallel circuit [5]**

Comparison between the case where the diode is not used and the case where the diode is connected in parallel is shown in Fig. 2-9 through Fig. 2-11 shows the left side is without diode, and the right side is with diode.

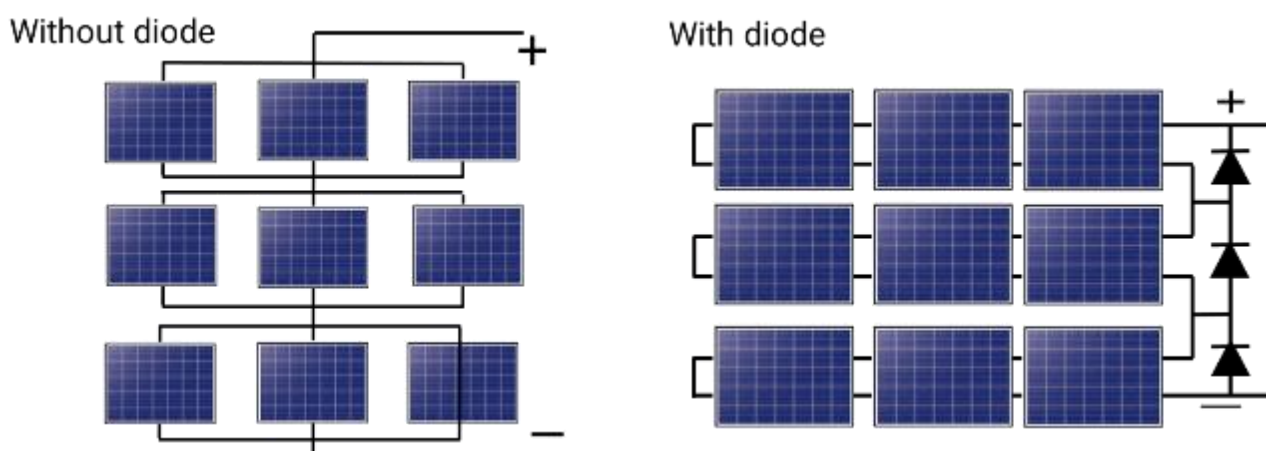


**Fig. 2-9 Series circuit and parallel diode circuit [5]**

The yellow line represents the current flow. Consider the case where two modules of the PV array are hidden behind and cannot generate electricity. Without diodes, the current will flow through all modules. On the other hand, if there is a diode, the current will flow to avoid modules that cannot generate electricity.

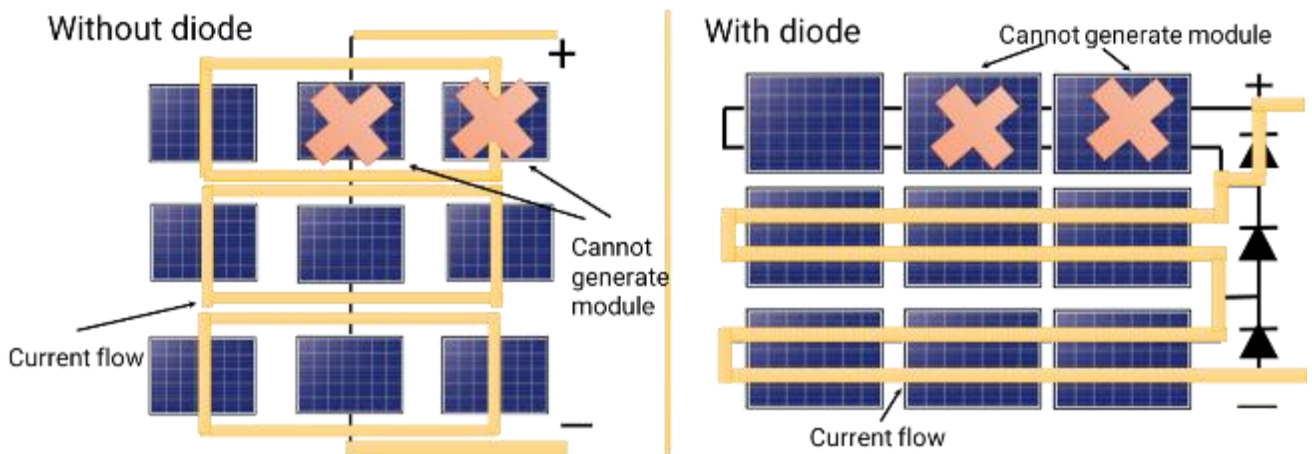


Fig. 2-10 PV-panel Partial shadow [5]

Without the diode, some modules couldn't generate electricity, which affected the whole thing. On the other hand, the whole was not affected when there was a diode because the current did not flow. This makes it possible to generate electricity more efficiently with the same number of modules.

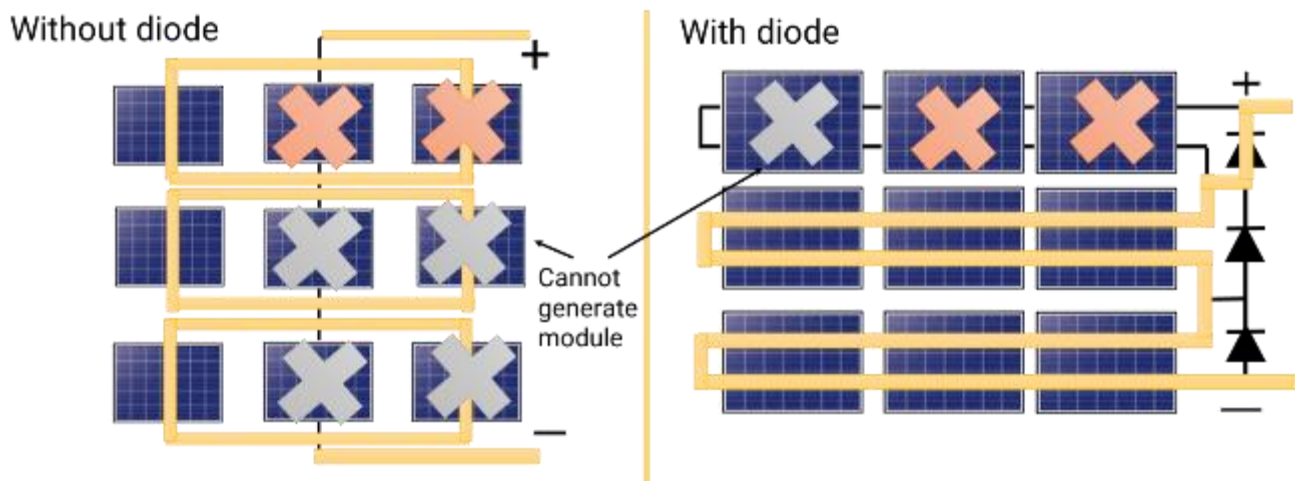


Fig. 2-11 Current flow in the partial shadow condition PV panel [5]

Fig. 2-12 is the equivalent circuit of the PV panel. This equivalent circuit contains 4 currents: Diode current, Ideal current, Series resistance, Parallel resistance. The relationship between them is expressed in Eq(2-1).

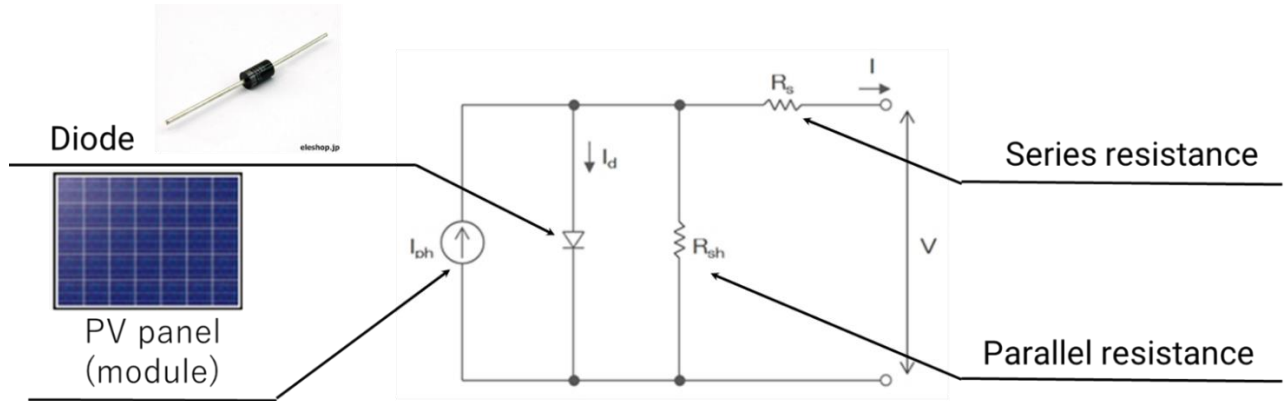


Fig. 2-12 Equivalent circuit of PEM panel [4]

$$I = I_{ph} - I_d - I_r \quad (2-1)$$

$I_{ph}$  is ideal current and  $I_d$  is diode current.  $I_r$  is parallel resistance current.

$$I_{ph} = I_{SC} \times \frac{G_{Total}}{G_{ref}} \times [1 + K_i \times (T_{cell} - T_{ref})] \quad (2-2)$$

$I_{SC}$  is short circuit current.  $G_{Total}$  is PEM radiation.  $G_{ref}$  is reference PEM radiation. This reference PEM radiation is  $1000[\text{W}/\text{m}^2]$ .  $K_i$  is temperature dependence of the short circuit current.  $T_{cell}$  is cell temperature.  $T_{ref}$  is reference cell temperature. The reference cell temperature is  $25^\circ\text{C}$ .

The diode current is calculated from Eq. (2-5).  $I_0$  is reverse saturation current. The reverse saturation current is decided by Eq (2-3).  $q$  is the electron charge. Eq (2-3) contain  $I_{0,STC}$ .  $I_{0,STC}$  is reverse saturation current at the standard test conditions. This number is decided by Eq (2-3).  $T_{cell}$  is cell temperature.  $E_{g0}$  is bandgap of PV material.  $V_{OC}$  is the open-circuit voltage.  $n$  is identified number. On the next Eq(2-3),  $k_B$  is Boltzman constant.  $R_s$  is series resistance of a PV cell.  $I_{SC}$  is short circuit current.

$$I_{0,STC} = \frac{I_{SC}}{\exp\left(\frac{q \times V_{OC}}{N_s \times k_B \times n \times T_{cell}}\right) - 1} \quad (2-3)$$

$$I_0 = I_{0,STC} \times \left(\frac{T_{cell}}{298}\right)^3 \times \exp\left[\frac{q \times E_{g0}}{n \times k_B} \times \left(\frac{1}{298} - \frac{1}{T_{cell}}\right)\right] \quad (2-4)$$

$$I_d = I_0 \times \left[ \exp\left( q \times \frac{\left(\frac{V}{N_s}\right) + I \times R_s}{n \times k_B \times T_{cell}} - 1 \right) \right] \quad (2-5)$$

$I_r$  is ohmic current.  $I_r$  is calculated by Eq(2-6).  $V$  is the output voltage.  $I$  is output current.  $R_s$  is the series resistance of a PV cell.  $R_{sh}$  is the shunt resistance of a PV cell.

$$I_r = \frac{V}{N_s} + I \times R_s \quad (2-6)$$

The output of the solar panel also changes with the surface temperature of the solar panel. The surface temperature of the solar panel can be calculated from Eq (2-7).  $T_{cell}$  is cell temperature.  $T_a$  is ambient temperature.  $G_T$  is solar radiation.  $T_{c,NOCT}$  is cathode side nominal operating temperature.  $T_{a,NOCT}$  is anode side nominal operating temperature.  $G_{T,NOCT}$  is nominal operating solar radiation.

$$T_{cell} = T_a + G_T \times \left( \frac{T_{c,NOCT} - T_{a,NOCT}}{G_{T,NOCT}} \right) \times (1 - \eta_{cell}) \quad (2-7)$$

The following flowchart shows the PV output current calculation steps explained by Eq (2-1) to Eq (2-7).

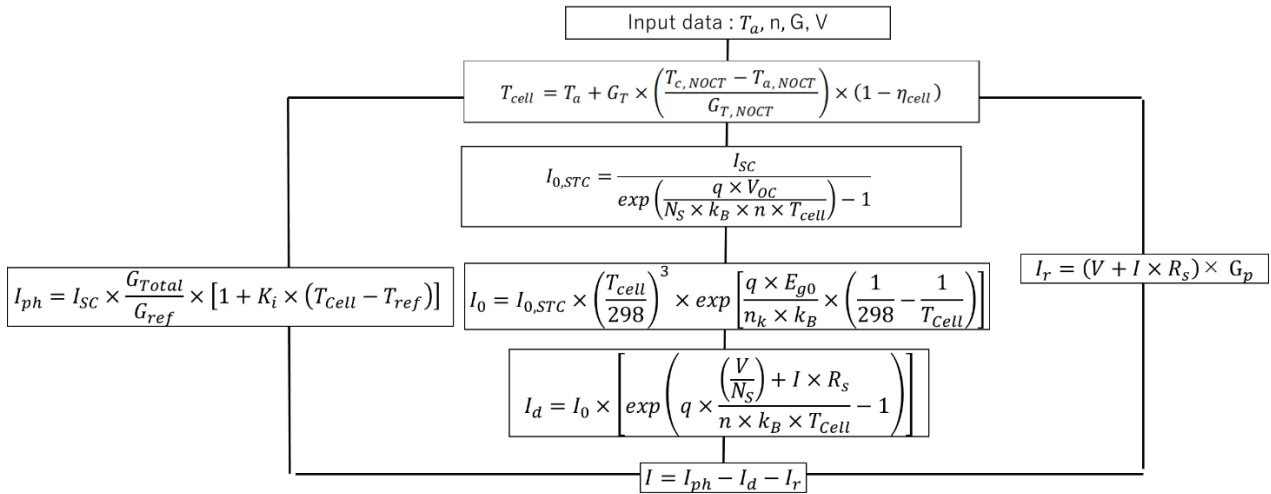


**Fig. 2-13 PV-panel output current calculation flowchart**

## 2.2. Basic concept of the Solar Electrolyzer

The Solar electrolytic cell is very similar to a solar fuel cell. Solar fuel cells consume hydrogen and produce energy. On the contrary, the solar electrolytic layer consumes energy and produces hydrogen. The solar electrolytic cell operates by the mechanism shown in Fig. 2-14. First, water is supplied from the diffusion layer on the anode side. Next, water is electrolyzed at the electrode on the anode side and separated into hydrogen ions and oxygen ions. The separated oxygen ions combine to form oxygen. Oxygen is discharged from the diffusion layer. Hydrogen ions pass through the electrolytic membrane. After adding the electrolytic membrane, the hydrogen ions combine to form hydrogen.

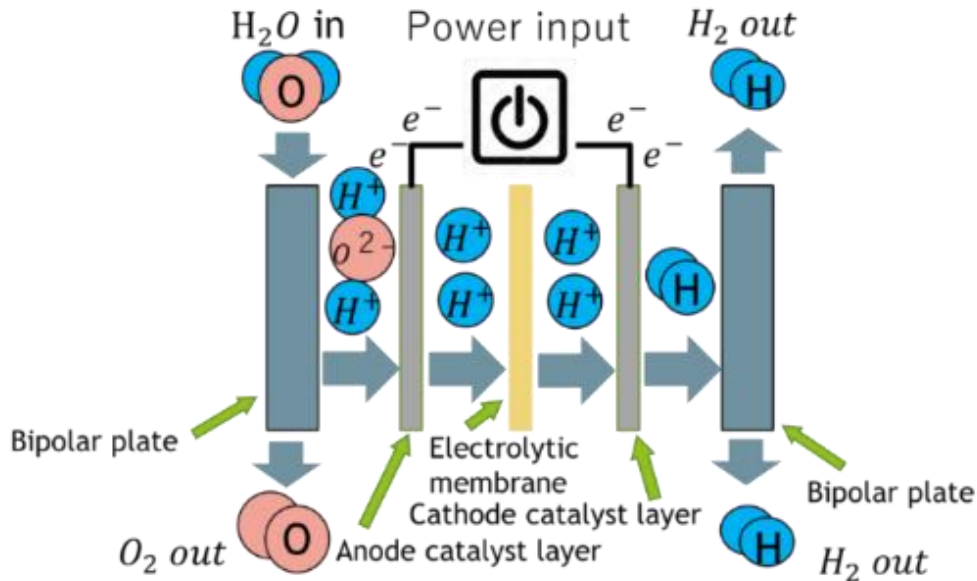


Fig. 2-14 Electrolyzer working mechanisms [3]

The electrolyzer's overall voltage is the sum of the four types of voltage.  $E$  is the open-circuit voltage.  $\eta_{ohm}$  is the anode side activation overvoltage.  $\eta_{ac,c}$  is the cathode side activation overvoltage.  $\eta_{ac,a}$  is the anode side activation overvoltage.  $\eta_{dif}$  is the concentration loss [18].

$$V = E + \eta_{ohm} + \eta_{ac,a} + \eta_{ac,c} + \eta_{dif} \quad (2-8)$$

The open-circuit voltage can be calculated by Eq. (2-9). The left side calculates the voltage used to separate water into hydrogen and oxygen. The right-hand side calculates the voltage used to change the volume and pressure of hydrogen and oxygen.  $\Delta G$  in Eq. (2-9) is the Gibbs free energy.  $F$  is the Faraday constant.  $R$  is the gas constant.  $T_{cell}$  is the cell temperature.  $a_{H_2O}$  is the partial pressure of water.  $P_{O_2}$  is the partial pressure of oxygen.  $P_{H_2}$  is the partial pressure of hydrogen.

$$E = -\frac{\Delta G}{2 \times F} + \frac{R \times T_{cell}}{2 \times F} \times \left[ \ln \left( \frac{P_{H_2} \times P_{O_2}^{\frac{1}{2}}}{a_{H_2O}} \right) \right] \quad (2-9)$$

Energy that separates water into oxygen and hydrogen
Energy used to change pressure and volume between hydrogen and oxygen

$\Delta G$ : Gibbs free energy in Eq. (2-9) can be calculated from Eq. (2-10).  $\Delta G$  can be calculated from the difference

between the potential energy of hydrogen and oxygen and the potential energy of water, as shown in Fig. 2-15. Also, not all energy is used to separate water molecules; some is converted to thermal energy.

$$\Delta G = \Delta H - (T-298) \times \Delta S \quad (2-10)$$

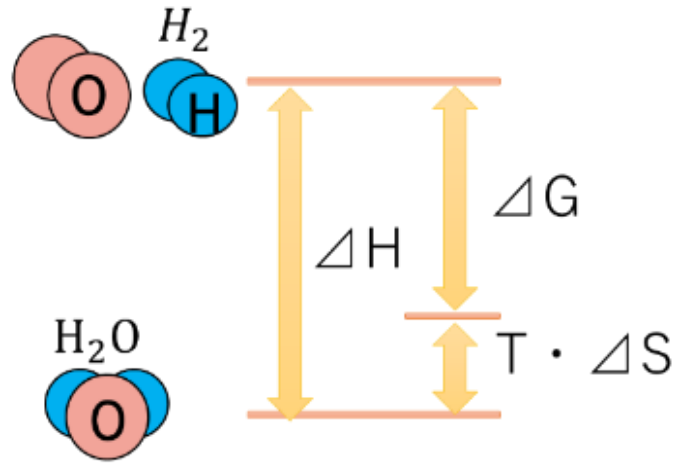


**Fig. 2-15 : Relationship between internal energy of water molecule, oxygen molecule, and hydrogen molecule**

The partial pressure of water in Eq. (2-11) can be calculated from Eq. (2-11) to Eq. (2-13).  $t$  is the temperature of the water during the reaction. This time,  $t$  is assumed to be the same as the cell temperature. Next,  $P_{O_2}$ , oxygen partial pressure, in Eq. (2-9) can be calculated from Eq. (2-12).  $P_{anode}$  represents the pressure on the anode side.  $P_{H_2}$ , in Eq. (2-11), is hydrogen partial pressure which can be calculated from Eq. (2-13).  $P_{cathode}$  represents the pressure on the cathode side.

$$a_{H_2O} = \frac{610}{1.0 \times 10^5} \times \exp\left[\frac{t}{t+238.3} \times 17.2694\right] \quad (2-11)$$

$$P_{O_2} = P_{anode} - a_{H_2O} \quad (2-12)$$

$$P_{H_2} = P_{cathode} - a_{H_2O} \quad (2-13)$$

$\eta_{ohm}$  represents ohm loss. The left side of Eq. (2-14) represents the electrical resistance of the electrodes on the anode and cathode sides.  $r_e$  is the sum of the resistance of the electrodes on the anode side and the cathode side.  $i$  is the current density. The right side is the electrical resistance of the electrolytic film.  $h_m$  is the electrolytic film thickness.  $\sigma_m$  is the conductivity of the electrolytic membrane.  $\sigma_m$ : The conductivity of the electrolytic film can be calculated from Eq. (2-15).  $\lambda_m$  represents the membrane humidification of the electrolytic membrane.  $T_m$  is the temperature of the electrolytic membrane.

$$\eta_{ohm} = r_e \times i + \frac{h_m \times i}{\sigma_m} \quad (2-14)$$

Anode and Cathode catalyst layer's resistance
Electrolytic membrane resistance



$$\sigma_m = [0.005139 \times \lambda_m - 0.00326] \exp \left[ 1268 \times \left( \frac{1}{303} - \frac{1}{T_m} \right) \right] \quad (2-15)$$

$\eta_{ac,a}$  is the voltage to activate the reaction on the anode side. R is the gas constant.  $T_a$  is the electrode temperature on the anode side. This time, it is assumed that  $T_a$ : the electrode temperature on the anode side and  $T_{cell}$ : the cell temperature is the same. F is the Faraday constant. i is the current density.  $i_{0,a}$  represents the exchange current density on the anode side.

$$\eta_{act,a} = \frac{R \times T_a}{2 \times F} \times \operatorname{arcsinh} \left( \frac{i}{2 \times i_{0,a}} \right) \quad (2-16)$$

$\eta_{ac,c}$  is the voltage to activate the reaction on the cathode side. R is the gas constant.  $T_c$  is the electrode temperature on the cathode side. This time, it is assumed that  $T_a$ : cathode side electrode temperature and  $T_{cell}$ : cell temperature is the same. F is the Faraday constant. i is the current density.  $i_{0,c}$  represents the exchange current density on the cathode side.

$$\eta_{act,c} = \frac{2 \times R \times T_a}{F} \times \operatorname{arcsinh} \left( \frac{i}{2 \times i_{0,c}} \right) \quad (2-17)$$

$\eta_{dif}$  is the concentration loss which is caused by the uneven flow in the diffusion layer, which can be calculated by Eq. (2-18). R is the gas constant.  $i_L$  is the current limit term. n is the number of electrons emitted by one water molecule. F is the Faraday constant.  $\alpha_{an}$  is the charge transfer coefficient.

$$\eta_{dif} = \frac{R \times T}{\alpha_{an} \times n \times F} \times \ln \left[ \frac{i_L}{i_L - i_{0,a}} \right] \quad (2-18)$$

Fig.2-16 shows the calculation steps of the output current of the solar electrolyzer system.

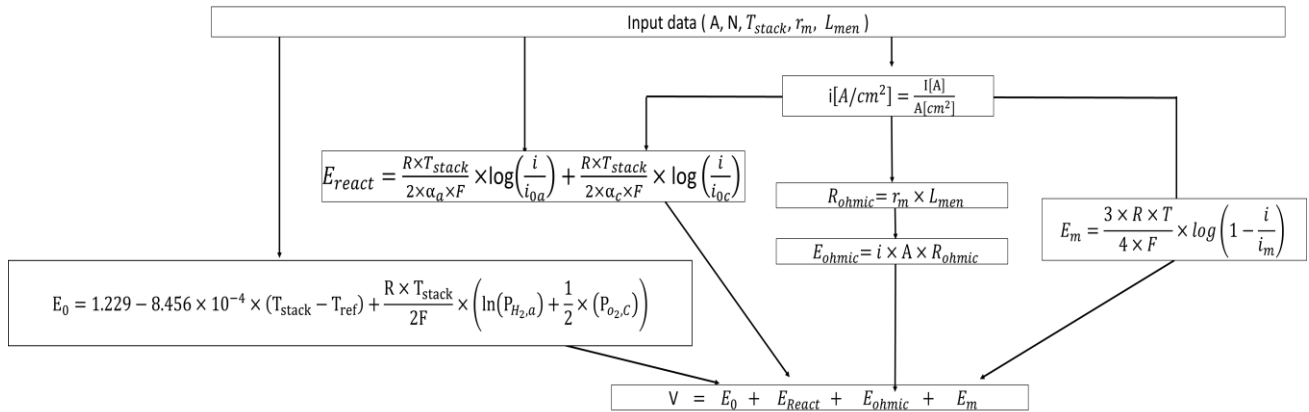


**Fig. 2-16 : Solar electrolyzer output current calculation flowchart**

The amount of hydrogen produced in the electrolytic layer was calculated from Eq. (2-19). This formula can calculate the amount of hydrogen generated per unit area per minute from the current density flowing through the electrolytic layer. i is the current density flowing through the electrolytic cell. F is the Faraday constant. N is the number of electrons emitted by one water molecule.  $\eta_F$  is the Faraday efficiency. R is the gas constant. P is 1 atmosphere (1013.15hpa). T is the operating temperature of the electrolytic layer.

$$Q_{H2,min} [\text{mL}/(\text{min} \cdot \text{cm}^2)] = \frac{i}{n \times F} \times \eta_F \times \frac{R \times T}{P} \times 60 \times 1000 \quad (2-19)$$

## 2.3. Basic concept of the Fuel cell model

The basic structure of a fuel cell is as shown in Fig. 2-17. First, hydrogen and oxygen are supplied to the fuel cell by the gas diffusion layer on the left and right sides. Hydrogen entering the fuel cell from gas diffusion layer is separated into hydrogen ions at the anode catalyst layer and emits electrons. The hydrogen ions generated at the anode catalyst layer move to the cathode catalyst layer through the electrolytic membrane. At this time, the electrons emitted by the anode catalyst layer are output to the outside through the copper wire. In the cathode catalyst layer, hydrogen ions and electrons are generated in anode catalyst layer, and oxygen flows through the gas diffusion layer, causing a chemical reaction to generate water. Fig 2-18 shows the reaction mechanism in a fuel cell. Then, the water generated at the cathode catalyst layer is discharged through the gas diffusion layer.

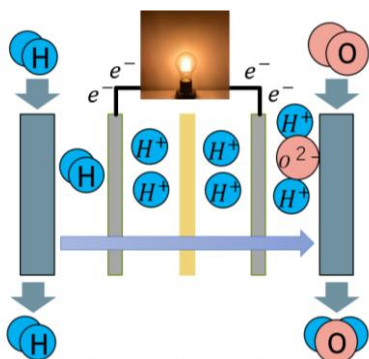
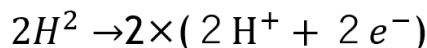
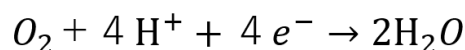


Fig. 2-17. Basic structure of a fuel cell [3]

Anode side



Cathode side



Overall chemical equation

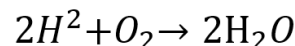


Fig. 2-18. Chemical reaction mechanism [3]

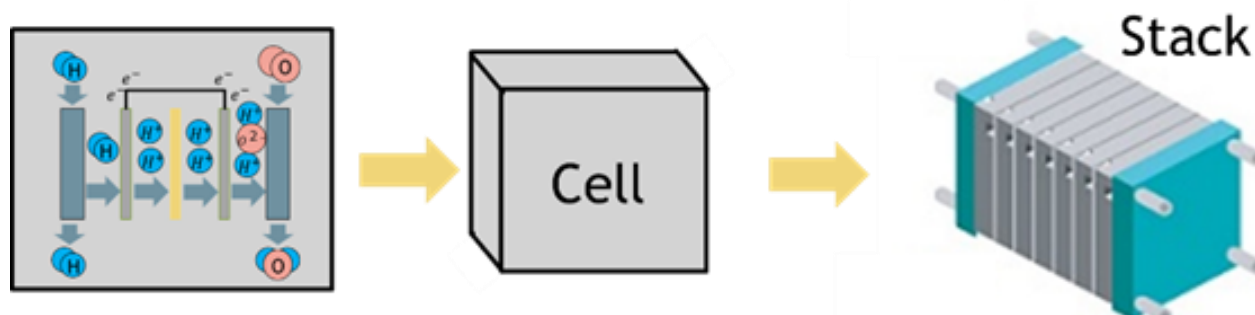


Fig. 2-19. Fuel cell stack [3]

Fuel cells operate by the mechanism shown in Fig. 2-17. One fuel cell shown in Fig. 2-17 is called a cell. However, this single cell cannot generate enough power. Therefore, as shown in Fig. 2-19, many cells are connected to form a mass called a stack. This is the same idea as the series connection of dry batteries shown in Fig. 2-20.

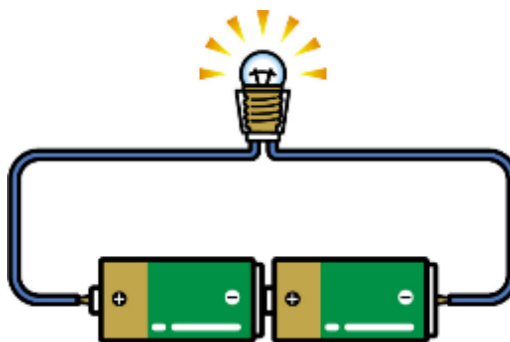


Fig. 2-20. Direct connection [3]

The output of the fuel cell can be expressed in electric power [W]. The power [W] is the product of the voltage [V] and the current [I], as shown in Eq. (2-20).

$$W(kw) = I \times V \quad (2-20)$$

And the current [A] can be calculated by multiplying the current density [ $i$ ] and the reaction area[A]. Then, the fuel cell outputs by combining the number of cells [N]. Therefore, the output of the stack can be calculated by the formula (2-21).

$$W(kw) = I \times V = N(-) \times A(cm^2) \times i(A/cm^2) \times V(V) \quad (2-21)$$

It was stated that the voltage could be calculated by the Eq (2-22). But this voltage is theoretical. In real, various losses occur, as shown in Eq. (2-23).

$$V = E_{cv} = E_0 - E_{React} - E_{ohmic} - E_m \quad (2-22)$$

$E_{cv}$  represents the actual voltage.  $E_0$  is called ideal voltage.  $E_{React}$  is called reaction loss.  $E_{ohmic}$  is called Ohmic loss.  $E_m$  is called concentration loss. [ $E_0$ ] can be obtained from the relational expression shown in Eq. (2-23).

$$E_0 = -\frac{\Delta G}{2F} - \frac{\Delta S}{2F} \times (T_{stack} - T_{ref}) + \frac{R \times T_{stack}}{2F} \times \left( \ln(P_{H_2,a}) + \frac{1}{2} \times (P_{O_2,c}) \right) \quad (2-23)$$

This  $E_0$  stands for the maximum voltage that can theoretically be output.  $n$  represents the number of electrons generated in the chemical reaction. As shown in Eq. (2-23), in the case of hydrogen, two electrons are emitted in the process of hydrogen replacing hydrogen ions. Therefore,  $n=2$ .

$n[-]$ :Exchanging electron of reaction

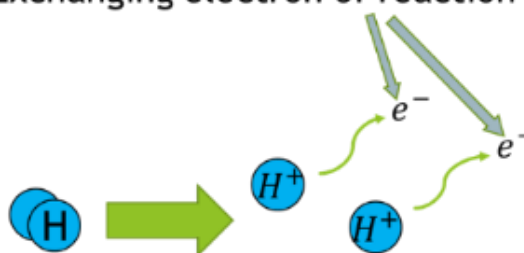


Fig. 2-21 Hydrogen chemical reaction

Reaction loss is the amount of energy that is released due to the chemical reaction and can be calculated by Eq. (2-24), Eq. (2-25).

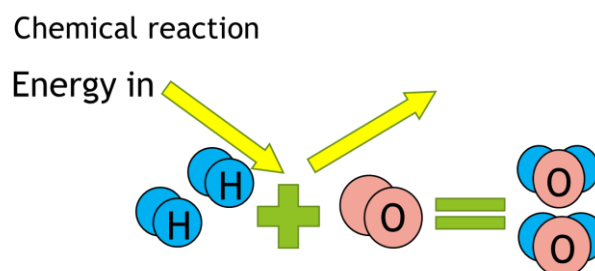


Fig. 2-22 Reacting loss

$$E_{React} = -\eta_1 - \eta_2 \times T - \eta_3 \times T \times \ln(C_{O_2}) - \eta_4 \times T \times \ln(I) \quad (2-24)$$

$$C_{O_2} = \frac{P_{O_2}}{5.08 \times 10^6 \times e^{\left(\frac{498}{T}\right)}} \quad (2-25)$$

**Tab. 2-1 Experimental values of  $\eta$  [18]**

$\eta_1$	0.944
$\eta_2$	$-3.54 \times 10^{-3}$
$\eta_3$	$-7.4 \times 10^{-4}$
$\eta_4$	$1.96 \times 10^{-4}$

Ohmic loss is the loss caused by the resistance of the electric membrane. This relationship can be applied Eq. (2-26). This resistance rate can change. The resistance rate can be calculated by Eq. (2-27).

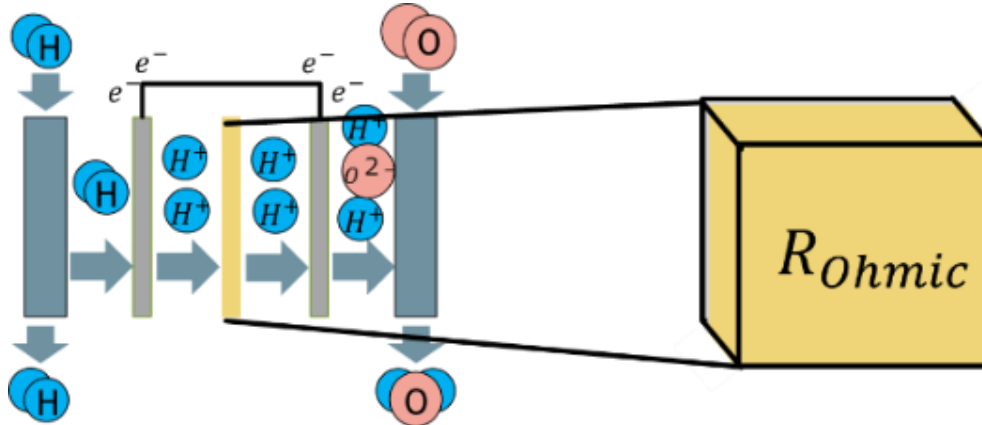


**Fig. 2-23 Ohmic loss**

$$E_{ohmic} = i \times R_{ohmic} = i \times l \times r_m \times L_{men} \dots \quad (3-8) \quad (2-26)$$

$$r_m = \frac{181.6 \times \left[ 1 + 0.03 \times \left( \frac{1}{A_{fc}} \right) + 0.062 \times \left( \frac{T}{303} \right)^2 \times \left( \frac{1}{A_{fc}} \right)^{2.5} \right]}{\left[ \lambda - 0.634 - 3 \times \left( \frac{i}{A} \right) \right] \times e^{\left[ \left( \frac{T-303}{T} \right) \right]}} \quad (2-27)$$

Concentration loss is caused by the difference in concentration of reactants on the electrode surface caused by fuel consumption. The concentration loss can be calculated from Eq. (2-28).

$$E_m = -\frac{3 \times R \times T}{4 \times F} \times \log \left( 1 - \frac{i}{i_m} \right) + 1.5607 \times \frac{R \times T}{4 \times F} \quad (2-28)$$

Fig. 2-24 shows the detailed calculation steps explained by Eq (2-20) to Eq (2-28).

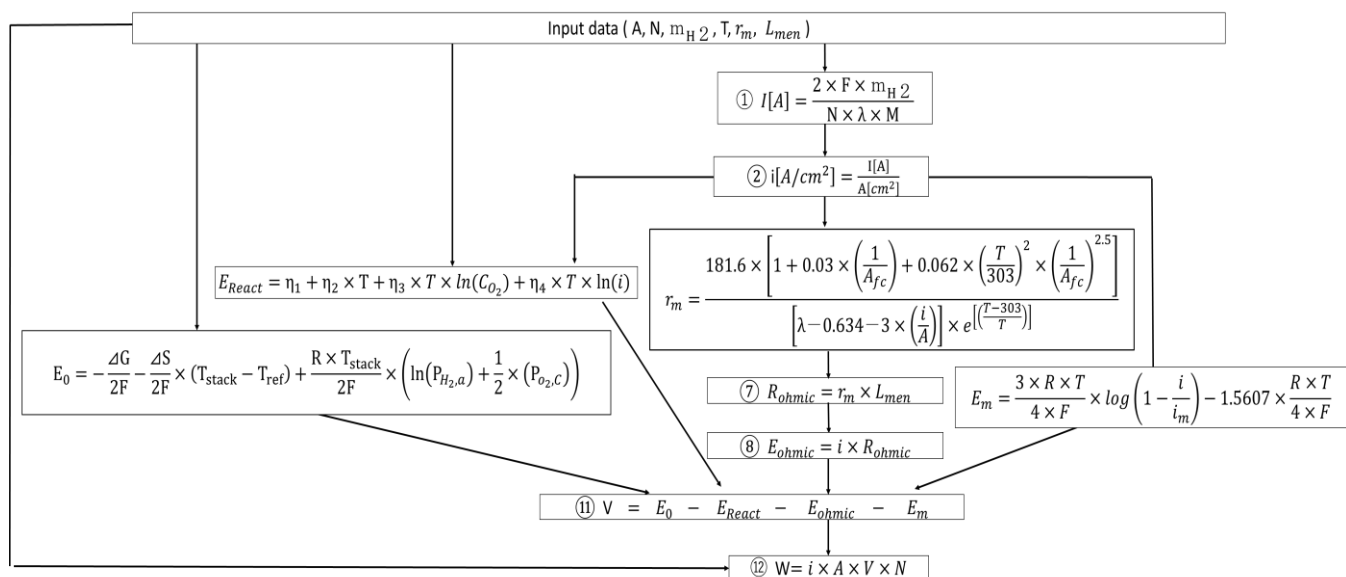


**Fig. 2-24 : Fuel cell power output calculation flowchart**

## 2.4. Model validation with the experimental data

The detailed calculation steps explained for the PV panel, solar electrolyzer, and fuel cell was performed in MATLAB software and validated with the reference experimental data as follows:

### 2.4.1. PV model test

Tab. 2-2 and Tab. 2-3 show the input data used to verify the PV panel simulation model.

**Tab. 2-2 Input data used in the PV model validation [6]**

Symbol	Value
$N_s$ : Number of cells	96 [-]
$K_i$ : Temperature dependence of the short circuit current	0.0538 [A/K]
$I_{sc}$ : Short-circuit current	6.07 [A]
$V_{oc}$ : Open-circuit Voltage	69.7[V]
$R_s$ : Series resistance	0.001 [ $\Omega$ ]
$R_{sh}$ : Parallel resistance	1000 [ $\Omega$ ]
n : ideality factor	1.2 [-]
$E_{g0}$ : Bandgap of PV material	1.1 [eV]

**Tab. 2-3 Range of input variables used in the PV model validation [6]**

Symbol	Value
G : Solar radiation	0~1000 [ $W/m^2$ ]
$T_a$ : Ambient temperature	24~31 [ $^{\circ}C$ ]

Fig. 2-25 represents the experimental measurement of the output current from the aforementioned solar panel in the range of 200 to 1000 [ $W/m^2$ ], which is compared with the results of the simulation model in Fig. 2-26, indicating the perfect agreement between the model results and measurement data.

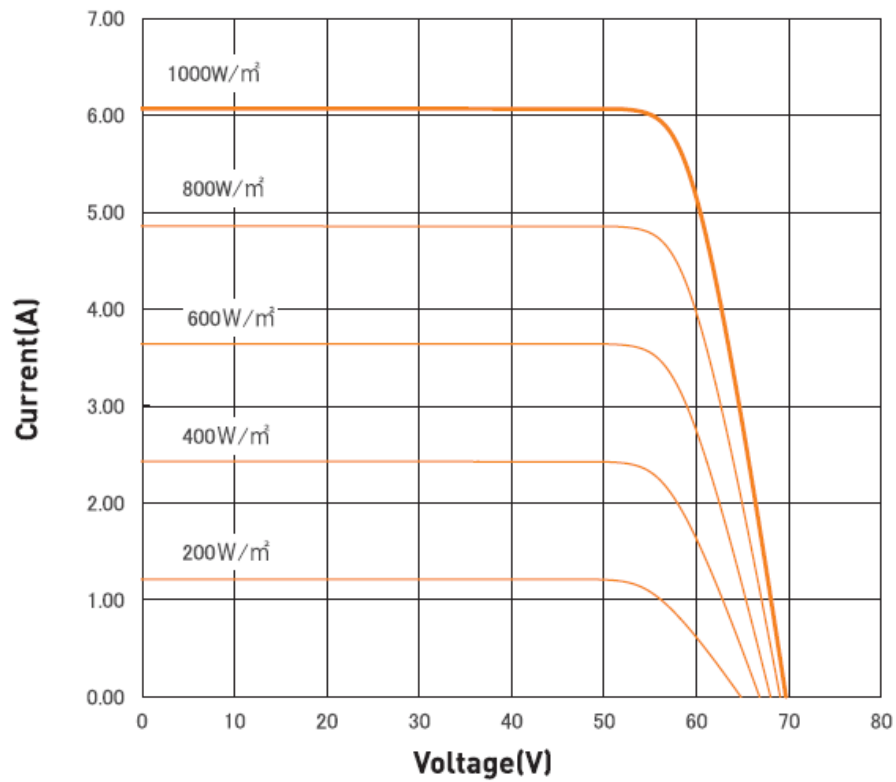


Fig. 2-25 Catalog I-V curve [6]

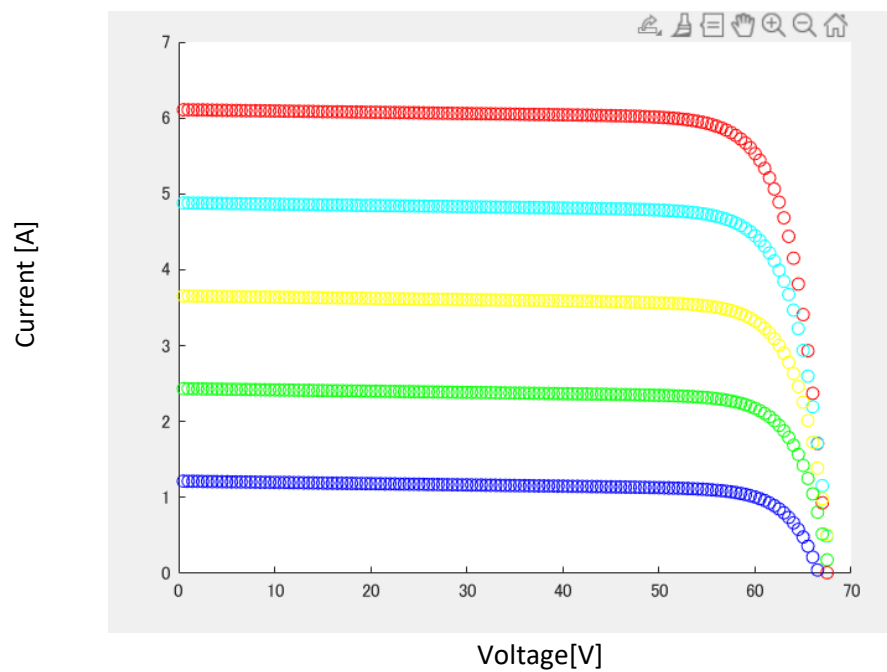


Fig. 2-26 MATLAB output I-V curve

## 2.4.2. Electrolyzer

Tab. 2-4 is the basic data of the electrolyzer used in HRES.

**Tab. 2-4 Input data used in the solar electrolyzer model validation [12]**

Symbol	Number
$i$ : Current density	0.00~0.35 [ $A/cm^2$ ]
$\eta_F$ : Faraday constant	1 [-]
<b>F</b> : Faraday constant	96485 [C/mol]
$n$ : Number of electrons	2 [-]
<b>R</b> : Gas constant	8.314 [J/(mol · K)]
<b>T</b> : Temperature	273.15 [K]
<b>P</b> : pressure	101300 [Pa]

Fig. 2-27 shows the comparison between the simulated (blue line) and measured (red dots) amount of hydrogen production, taking into account the same range for the input current to the solar electrolyzer.

Hydrogen product [ml/min]

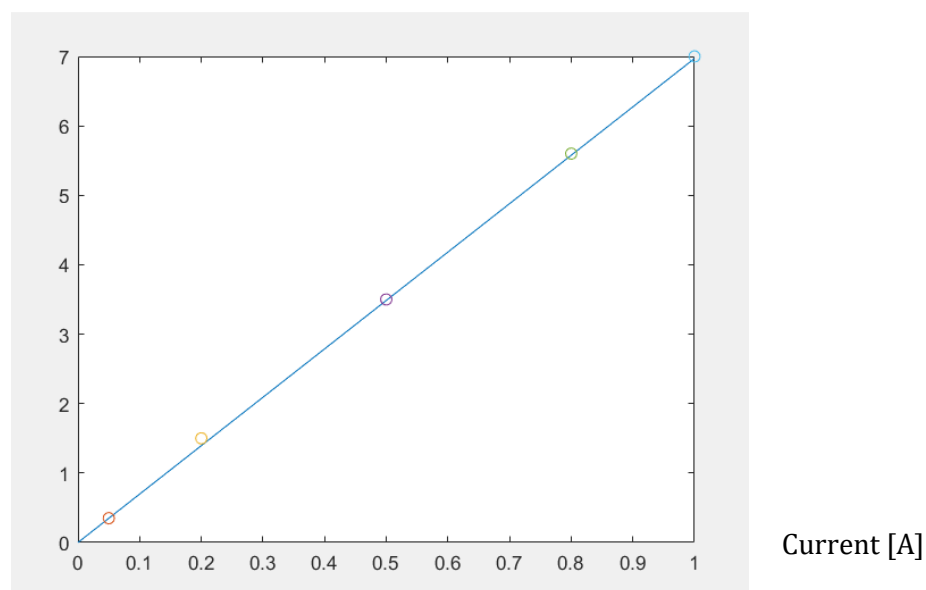



**Fig. 2-27 : Electrolyzer hydrogen output production rate**

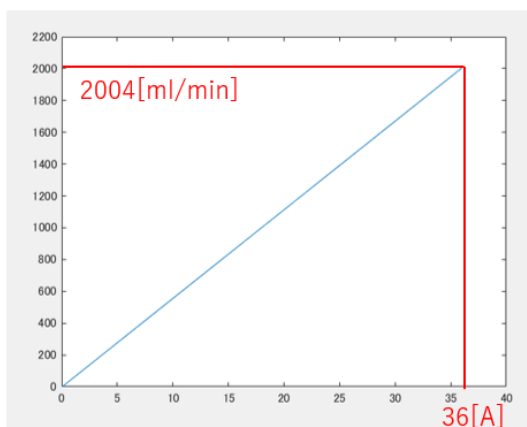
The simulation model was applied to a real commercial electrolyzer in the market to examine the relationship between voltage and current as well as hydrogen production rate and input current, as shown in Fig. 2-28 and Fig. 2-29. According to Tab. 2-5, the maximum rate of hydrogen production is achieved at 36 [A], which is about 2020 [ml/min]. While, based on the simulation model, this value is estimated at 2004 [ml/min], which confirms the very high accuracy of the model. The input current and voltage are estimated at 16.04 [V], 36 [A], which is very close to the technical data of the electrolyzer.



Tab. 2-5 Electrolyzer's basic input data [15]

Titan EZ-2000	
	
Out put flow rate	0~2020 [ml/min]
Input volt	16 [V]
Input amp	0~36 [A]
Number of cell	8 [-]
Reaction area	50 [cm <sup>2</sup> ]

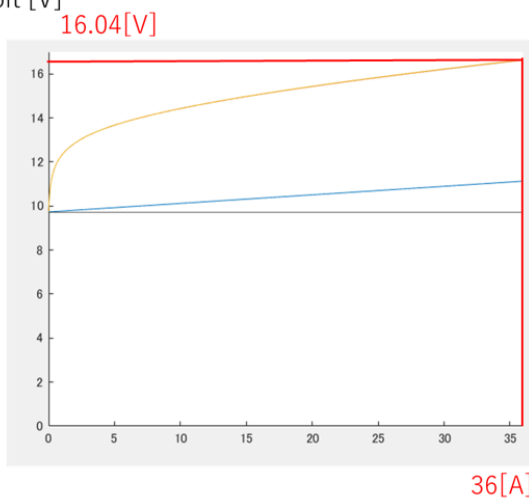
H2 output [ml/min]



Current : [A]

Fig. 2-28 Titan EZ-2000 I-H<sub>2</sub> curve

Volt [V]



Current : [A]

Fig. 2-29 Titan EZ-2000 I-V curve

## 2.4.3. Fuel cell

Fig. 2-30 shows the experimental setup of the PEM fuel cell installed at the Energy and Environmental Systems laboratory, Kyushu University. This experiment aims to find the I-V curve and I-W curve of the fuel cell. Tab. 2-6 shows the technical specification of the experimental setup.

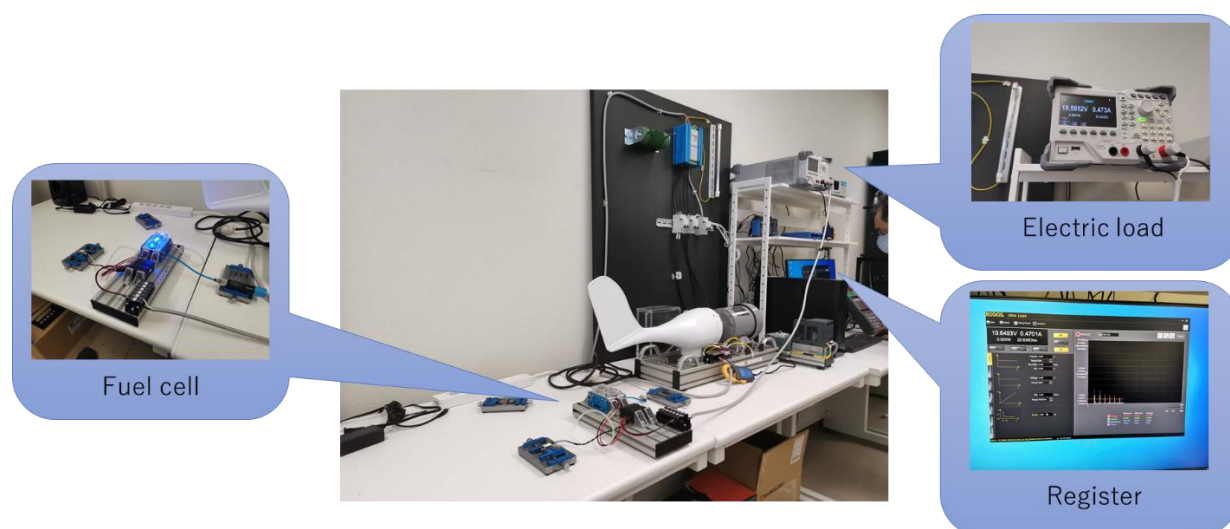


Fig. 2-30 Fuel cell experimental set up

Tab. 2-6 Technical specifications [14]


	Horizon H-30
	
A : Reaction area	7[ $\text{cm}^2$ ]
N : Number of cells	14[-]
mH <sub>2</sub> : Hydrogen flow rate	0.42 [L/min]
L <sub>men</sub> : Membrane thickness	20[ $\mu\text{m}$ ]
T : Temperature	0~55 [°C]
$P_m$ : Maximum power output	30 [W]
$I_m$ : Maximum power point current	3.6 [A]
$V_m$ : Maximum power point voltage	8.4 [V]

Fig. 2-31 to Fig. 2-33 represent the main characteristic curves of the fuel cell used in the experimental setup. Fig 2-34 to 2-36 show the graphs extracted based on the simulation results and the values obtained in the experiment, and the catalog [19]. The blue line is the simulation results. The red dots represent the values obtained in the experiment or collected from the catalog [19]. It can be observed from Fig. 2-34, that the values of the simulation result and the experimental measurement doesn't match each other in the range of the low current value. This is probably due to the low accuracy of the voltmeter at the time of the experiment. On the contrary, in the range where the current value is considerable, it can be seen that the agreement rate between the experimental result and the calculated result is very high. The simulation model results compared with the technical characteristic curves (hydrogen-power) and (power-current), which indicates the high accuracy of the simulation model.

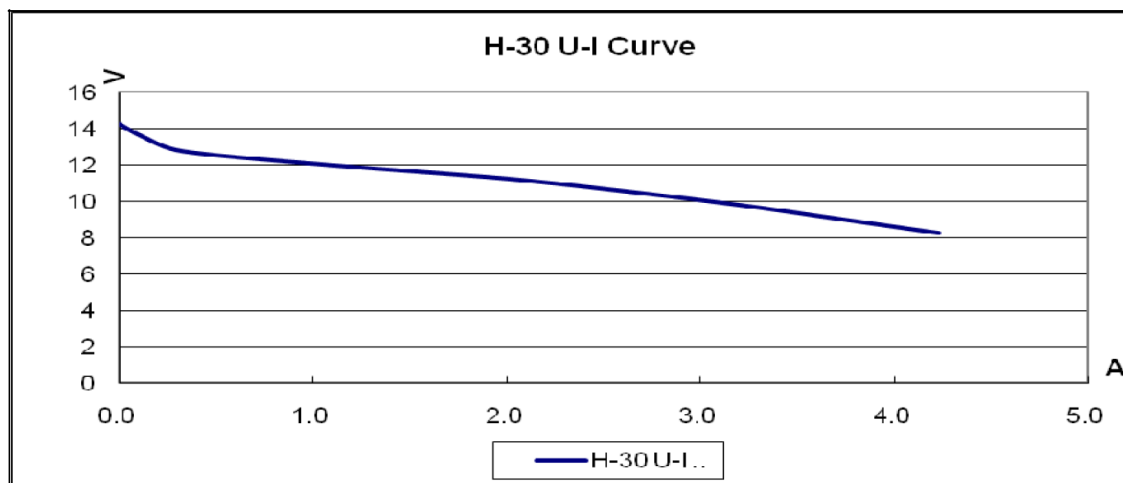


Fig. 2-31 Reference I-V curve [19]

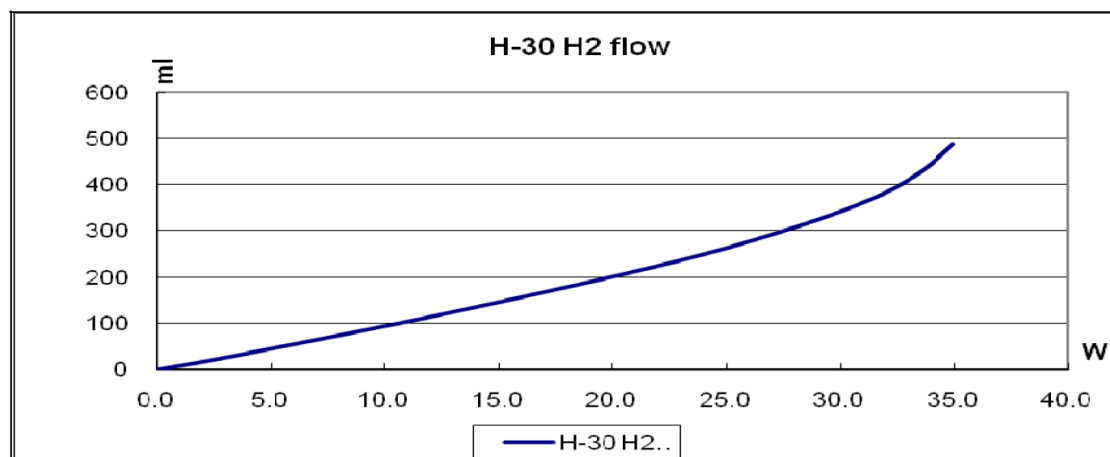


Fig. 2-32 Reference W-H2 curve [19]

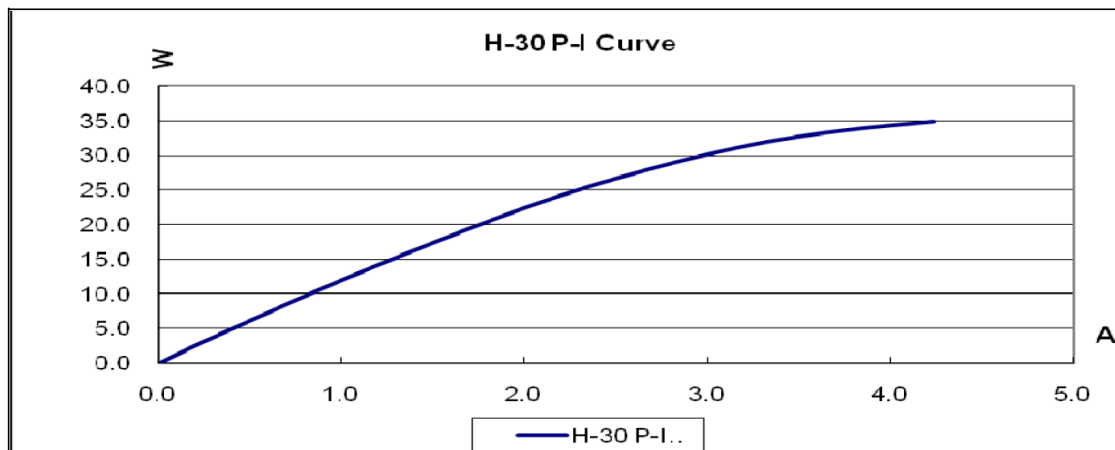


Fig. 2-33 Reference I-W curve [19]

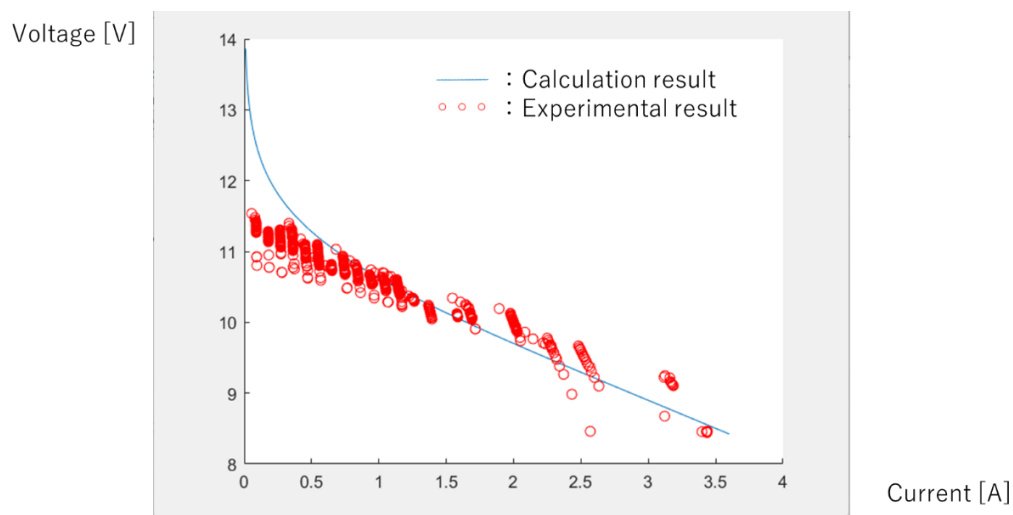


Fig. 2-34 Experimental and calculated I-V curve

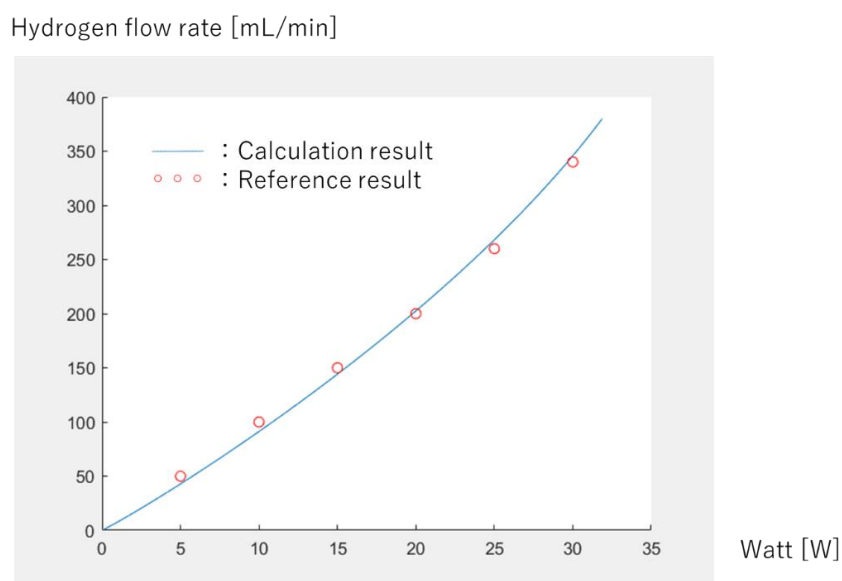
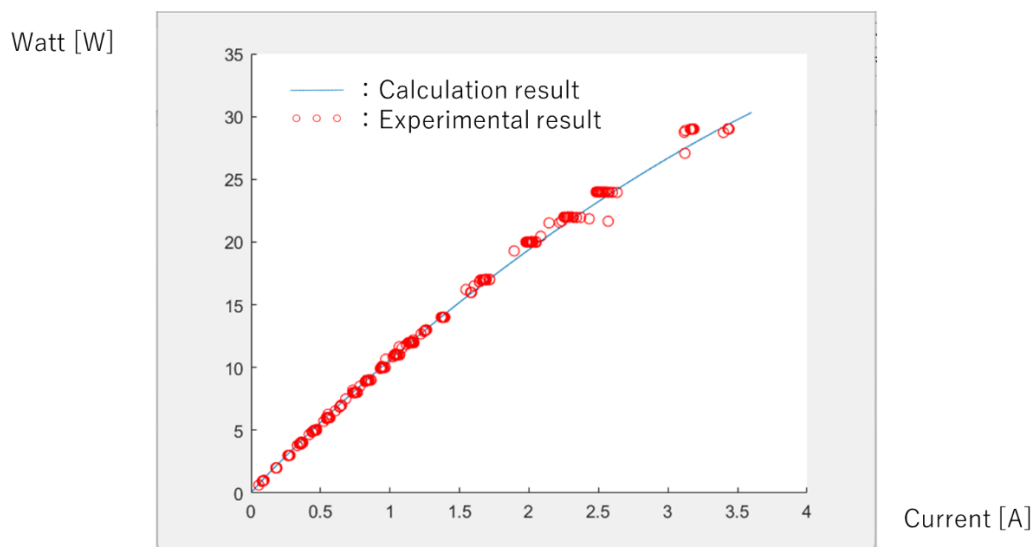



Fig. 2-35 Reference and calculated I-V curve



**Fig. 2-36 Experimental and calculated I-W curve**

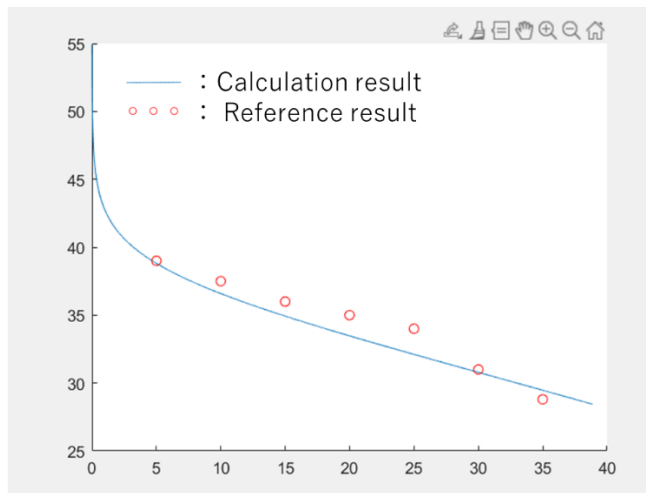
Since, a 30W fuel cell is small and cannot be used to power a household, therefore, the accuracy of the simulation model was also confirmed with a commercial fuel cell of 1000 W, which its specification is given in Tab. 2-7.

**Tab. 2-7 Basic data of fuel cell**

	Horizon H-1000
	
A : Reaction area	72[cm <sup>2</sup> ]
N : Number of cells	48[-]
mH <sub>2</sub> : Hydrogen flow rate	13 [L/min]
L <sub>men</sub> : Membrane thick ness	20[μm]
T : Temperature	0~65 [°C]
$P_m$ : Maximum power output	1000 [W]
$I_m$ : Maximum power point current	35 [A]
$V_m$ : Maximum power point voltage	28.8 [V]

The comparison between the simulation result and characteristic technical curves of 1000 W fuels cell is represented in Fig. 2-37 to Fig. 2-39.

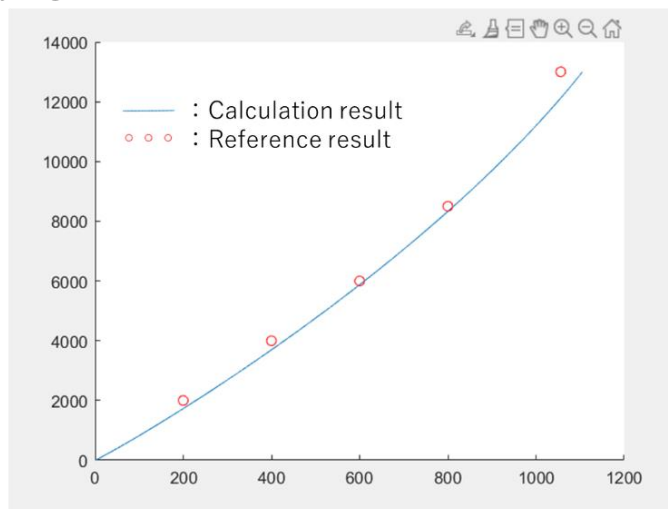
Voltage [V]



Current [A]

**Fig. 2-37 Experimental and calculated I-V curve**

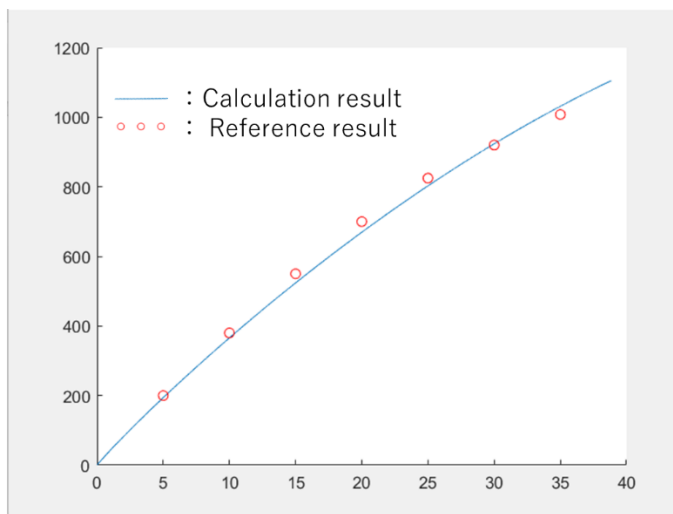
Hydrogen flow rate [mL/min]



Watt [W]

**Fig. 2-38 Reference and calculated I-V curve**

Watt [W]



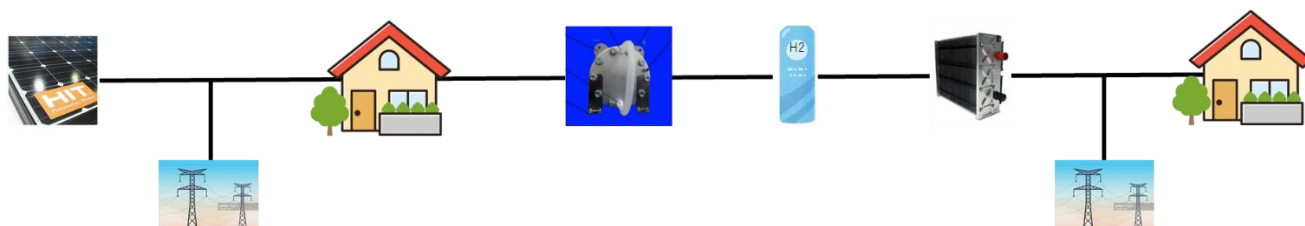
Current [A]

**Fig. 2-39 Experimental and calculated I-W curve**

### 3. Detailed design of the HRES

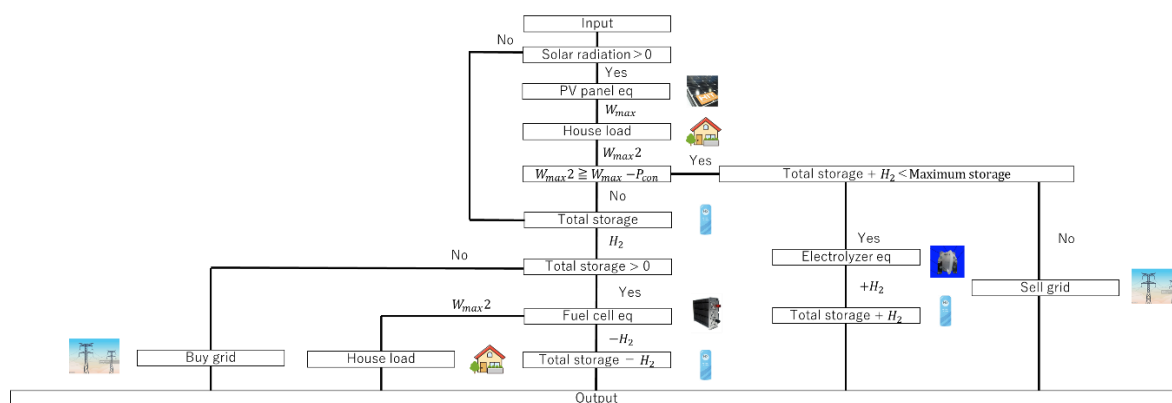
#### 3.1.HRES control strategy

Fig. 3-1 is the conceptual diagram of HRES. This system uses PV panels to generate electricity and supply it to the residential building. And if the solar panel alone does not have enough power, it will be provided from the grid. The surplus electricity supplied to the house is supplied to the electrolyzer to produce hydrogen. This hydrogen is stored in hydrogen storage. Hydrogen in hydrogen storage is fed to fuel cells to generate electricity during the night.



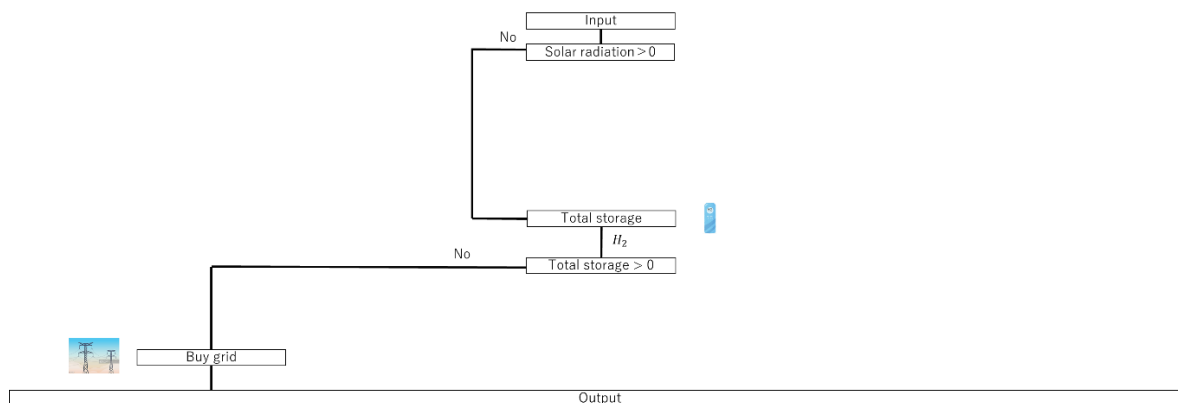
**Fig. 3-1 Proposed hydrogen-based HRES**

The control logic developed for the electricity and hydrogen generation and consumption is shown in Fig. 3-2.



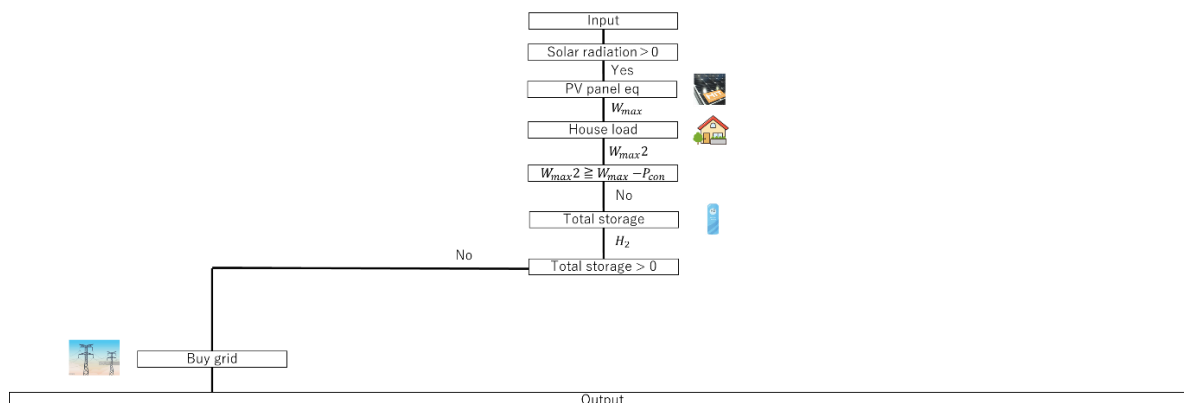
**Fig. 3-2 Overall control logic of the HRES**

According to the above control system, the HRES owner purchases electricity from the grid when sunlight is not available, and the amount of hydrogen in the storage is not enough to run the fuel cell



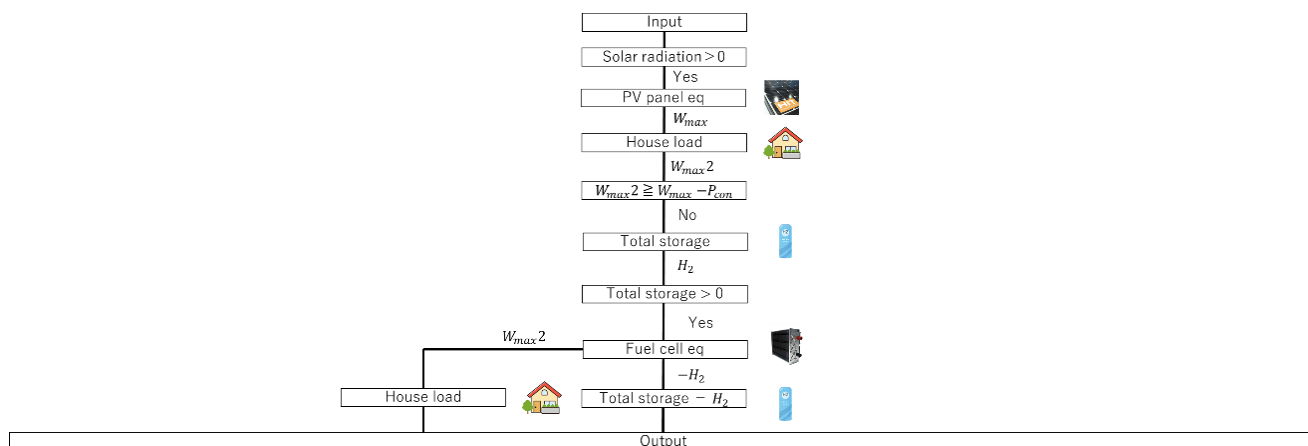
**Fig. 3-3 Purchasing electricity from the grid when sunlight and hydrogen are not available**

Fig. 3-4 shows the cloudy day condition; the solar radiation is not strong enough in order to fill the hydrogen tank, then the owner will decide to purchase electricity from the grid.



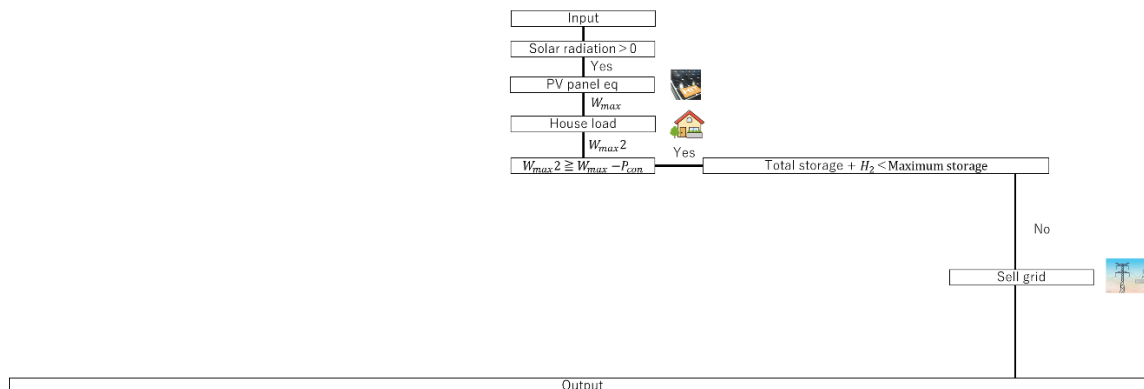
**Fig. 3-4 Low sunlight with empty hydrogen storage condition**

Fig. 3-5 shows a situation where the solar energy is not sufficient, but the hydrogen storage was sufficiently filled with hydrogen before, which is used in the fuel cell to meet the demand load requirements



**Fig. 3-5 Low sunlight, hydrogen storage available**

Fig. 3-6 shows the condition when the sunlight is strong and hydrogen storage is full. The HRES first generates electricity from solar panels and supplies electricity. Next, surplus electricity will be sold to the grid.



**Fig. 3-6 Hight sunlight, hydrogen storage is full**



### 3.2. Demand load profile

Fig. 3-7 shows the hourly electricity load in a typical Japanese residential building in January, April, July, and October, used in this research. Tab. 3-1 is a table that shows the hourly power consumption of a typical Japanese household every month. The electricity generated by the proposed HRES should meet the demand load requirement over one year. Electricity consumption basically increases from around 6:00 AM to 12:00 PM regardless of the season. Also, looking at the electricity consumption by month, January has the highest power consumption overall. April and July have the same electricity consumption, and October has the highest demand. This seems to be primarily related to the temperature of each month. For example, the temperature is low in January, and heating systems are used, so electricity consumption is high. On the other hand, October, when electricity consumption is the lowest, is a comfortable temperature throughout the day. As a result, it seems that power consumption has decreased.

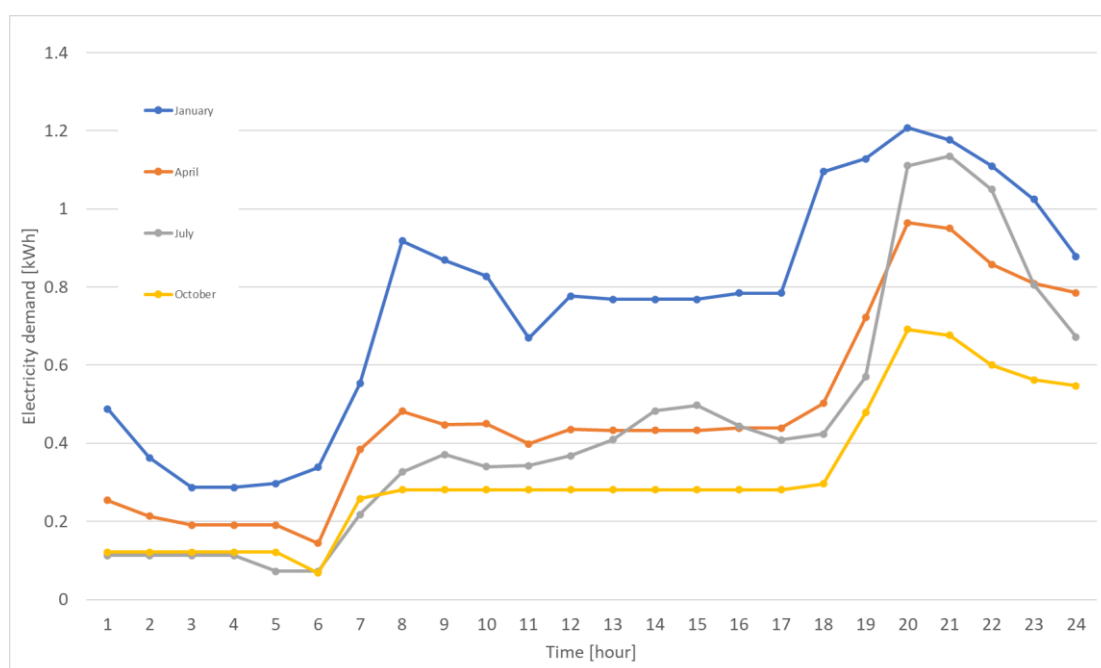


Fig. 3-7 Hourly electricity consumption in a typical Japanese house in this research

Tab. 3-1 Demand load of a typical residential building in Japan

	Jan	Feb	Mar	Apr	May	Jun	Jul	Aug	Sep	Oct	Nov	Dec
0	0.488	0.456	0.416	0.254	0.123	0.093	0.113	0.133	0.113	0.122	0.252	0.386
1	0.363	0.340	0.311	0.213	0.123	0.093	0.113	0.133	0.113	0.122	0.208	0.288
2	0.287	0.269	0.247	0.190	0.123	0.093	0.113	0.133	0.113	0.122	0.182	0.228
3	0.287	0.269	0.247	0.190	0.123	0.093	0.113	0.133	0.113	0.122	0.182	0.228
4	0.297	0.279	0.256	0.190	0.123	0.058	0.072	0.086	0.071	0.122	0.182	0.236
5	0.338	0.317	0.290	0.144	0.069	0.058	0.072	0.086	0.071	0.068	0.143	0.269
6	0.553	0.520	0.477	0.384	0.262	0.185	0.218	0.256	0.223	0.258	0.364	0.441
7	0.918	0.862	0.789	0.482	0.285	0.262	0.326	0.390	0.319	0.281	0.467	0.730
8	0.869	0.818	0.751	0.447	0.285	0.293	0.371	0.446	0.358	0.281	0.429	0.693
9	0.828	0.778	0.714	0.450	0.285	0.261	0.340	0.414	0.319	0.281	0.432	0.659
10	0.670	0.632	0.581	0.399	0.285	0.261	0.343	0.417	0.320	0.281	0.375	0.536
11	0.777	0.730	0.671	0.436	0.285	0.273	0.368	0.453	0.335	0.281	0.416	0.619
12	0.768	0.723	0.664	0.433	0.285	0.293	0.409	0.508	0.362	0.281	0.413	0.613
13	0.768	0.723	0.664	0.433	0.285	0.327	0.483	0.610	0.407	0.281	0.413	0.613
14	0.768	0.723	0.664	0.433	0.285	0.331	0.498	0.632	0.412	0.281	0.413	0.613
15	0.785	0.738	0.678	0.439	0.285	0.307	0.444	0.558	0.381	0.281	0.419	0.626
16	0.785	0.738	0.678	0.439	0.285	0.288	0.408	0.510	0.356	0.281	0.419	0.626
17	1.095	1.030	0.946	0.502	0.301	0.297	0.424	0.530	0.368	0.296	0.486	0.873
18	1.128	1.061	0.973	0.722	0.486	0.423	0.570	0.699	0.520	0.479	0.686	0.899
19	1.208	1.136	1.044	0.965	0.702	0.775	1.111	1.390	0.960	0.691	0.905	0.964
20	1.176	1.106	1.015	0.950	0.687	0.776	1.135	1.429	0.964	0.676	0.893	0.938
21	1.110	1.043	0.958	0.858	0.609	0.730	1.050	1.316	0.905	0.600	0.808	0.885
22	1.024	0.962	0.882	0.809	0.571	0.598	0.805	0.989	0.735	0.562	0.763	0.815
23	0.878	0.824	0.754	0.785	0.555	0.494	0.672	0.828	0.608	0.547	0.741	0.698

### 3.3. Solar incident on the tilted PV surface:

The receiving solar radiation on the PV panel is defined based on the spherical coordinate system and ambient condition in each location which is shown in Fig.3-8.  $S_{incident}$  stands for the incident solar radiation.  $S_{horizontal}$  refers to horizontal solar radiation. Horizontal solar radiation is the amount of solar radiation that falls perpendicular to the ground from the sun.  $S_{module}$  represents module solar radiation. Module solar radiation is the solar radiation that falls perpendicular to the PV panel, which is calculated through Eq (3-1) to Eq (3-4)

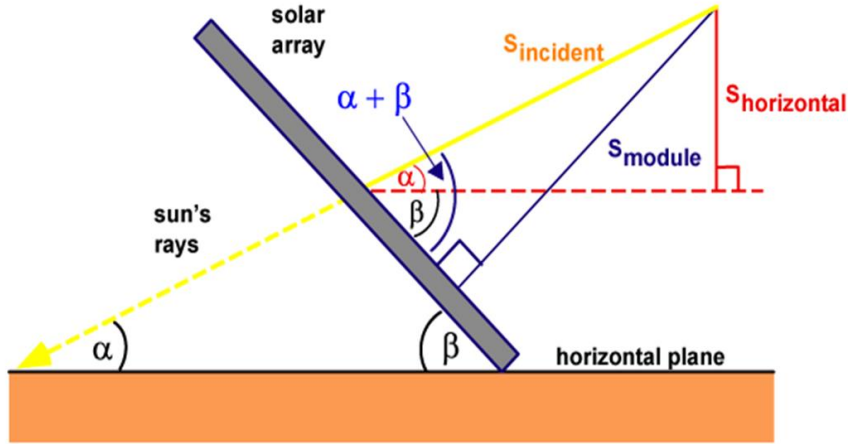


Fig. 3-8 Demonstration of the incident solar radiation on tilted PV panel [4]

$$S_{horizontal} = S_{incident} \times \sin\alpha \quad (3-1)$$

$$\alpha = 90 - \Phi + \delta \quad (3-2)$$

$$\delta = 23.45 \times \sin \left[ \left( \frac{360}{365} \right) \times (284 + d) \right] \quad (3-3)$$





In the above equations,  $\alpha$  is calculated by Eq (3-2).  $\Phi$  is latitude.  $\delta$  is declination angle. Finally, the incident solar radiation on the PV module can be calculated as follows:

$$S_{module} = S_{incident} \times \sin(\alpha + \beta) \quad (3-4)$$

### 3.4. HRES size estimation

Tab. 3-2 shows the quantity and size of each element of the HRES which is supposed to satisfy the demand load given in Tab 3-1.

**Tab. 3-2 quantity and size of the HRES components**

Each component	PV-panel	Electrolyzer	Fuel cell	Hydrogen storage
				
Each component detail	VBHN330SJ47-1[m <sup>2</sup> ]	Titan EZ-2000	Horizon H-1000	
Number of components	28[-]	8[-]	2[-]	7000[L]

For this HRES, it is assumed that 1 square meter of Panasonic model type “VBHN330SJ47” is used to be easily applied to various conditions, as shown in Fig. 3-9. However, this model does not have a 1 square meter model. So, it needs to predict the output of 1 square meter based on the manufacturer's catalog.

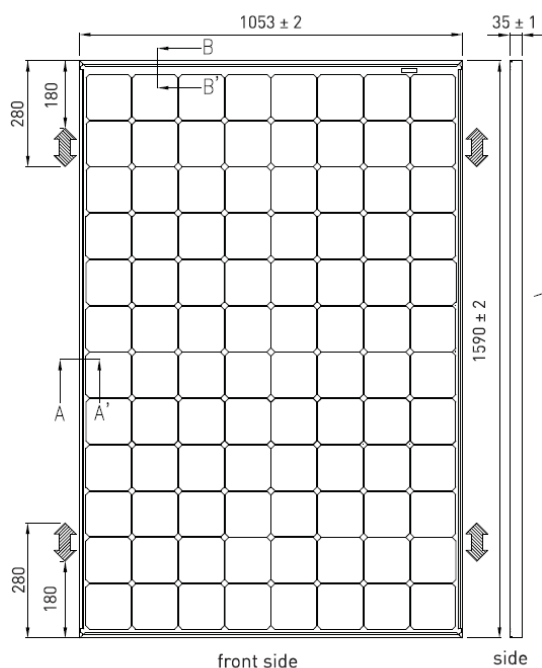


**Fig. 3-9 Surface of Panasonic VBHN330SJ47 [6]**

$N_{1.67}$  is the number of cells per 1.67 [m<sup>2</sup>] solar panel. Next, the number of cells of the 1.0 [m<sup>2</sup>] solar panel is 8 [-] vertically and horizontally, and the number of cells per 1.0 [m<sup>2</sup>] solar panel is 64 [-]. increase. Let  $N_{1.0}$  be the number of cells per 1.0 [m<sup>2</sup>] solar panel. Each cell is square and connected in series. In this case, the output voltage of the 1.67 [m<sup>2</sup>] solar panel is  $V_{1.67}$  [V], the output current is  $I_{1.67}$  [A], the output power is  $W_{1.67}$  [W], and then 1.0 [m<sup>2</sup>] Let the output voltage of the solar panel in 2) be  $V_{1.0}$  [V], the output current be  $I_{1.0}$  [A], and the output power be  $W_{1.0}$  [W]. Calculate  $V_{1.0}$  [V],  $I_{1.0}$  [A],  $W_{1.0}$  [W] from the above conditions. The voltage is proportional to the number of cells in the solar panel.  $V_{1.0}$  [V] can be calculated from [Eq. 2-32].

$$V_{1.0}[V] = V_{1.67}[V] \times \frac{N_{1.0}[-]}{N_{1.67}[-]} \quad (3-5)$$

The current is proportional to the surface area of the solar panel.  $A_{1.67} [m^2]$  is the surface area per PV-cell of a 1.67  $[m^2]$  solar panel. Next,  $A_{1.0} [m^2]$  be the surface area per cell of the 1.0  $[m^2]$  solar panel. Fig. 3-10 show each PV-panel surface area of one cell.  $A_{1.67}$  was decided to be 0.017325  $[m^2]$ . And,  $A_{1.0}$  was decided to be 0.015625  $[m^2]$ .

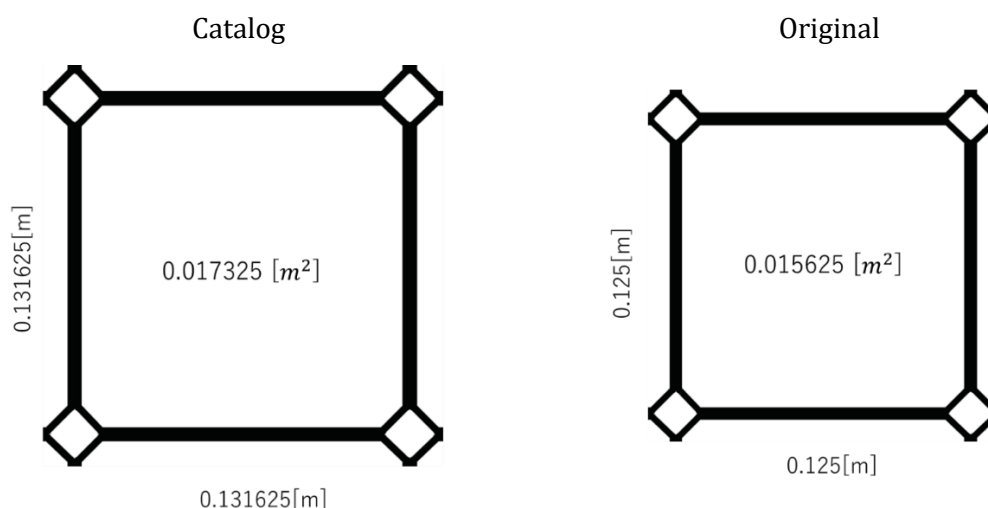


**Fig. 3-10 Surface area of one cell [6]**

The calculated current of 1 square meter PV-panel is as follows:

$$I_{1.0}[A] = I_{1.67}[V] \times \frac{A_{1.0}[-]}{A_{1.67}[-]} \quad (3-6)$$

From Eq (3-5) and Eq (3-6) were able to calculate the current, voltage, and power of a 1  $[m^2]$  solar panel. Tab. 3-3 summarizes the catalog data and the 1  $[m^2]$  solar panel data.

**Tab. 3-3 Modified PV-panel basic data [6]**



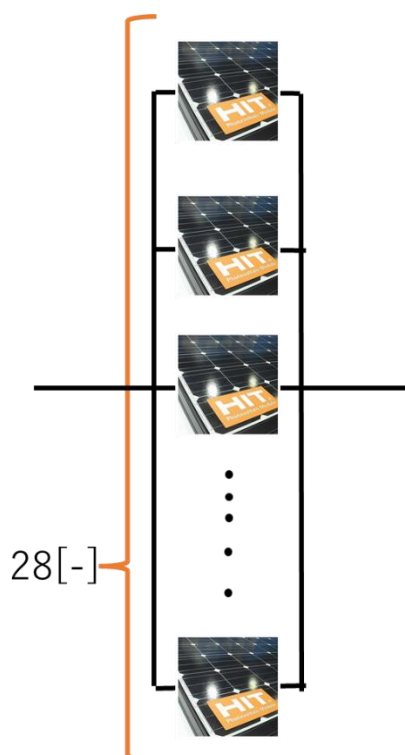
	Panasonic VBHN330SJ47	
	Reference data	Original data
		
A : PV-panel surface area	1.674 $[m^2]$	1.0 $[m^2]$
$A_{1.67}, A_{1.0}$ : PV-panel one cell surface area	0.017325 $[m^2]$	0.015625 $[m^2]$
$N_{1.67}, N_{1.0}$ : Number of cells	96 [-]	64 [-]
$I_{max}$ : Maximum power point current	5.7 [A]	5.19 [A]
$V_{max}$ : Maximum power point voltage	58.0 [V]	38.7 [V]
$W_{max}$ : Maximum power point power output	330 [W]	198 [W]


Fig. 3-11 shows the connection diagram of a 1 square meter solar panel. Twenty-eight solar panels were connected in parallel.



**Fig. 3-11 Solar panel connection diagram**

Tab. 3-4 shows the specifications of the electrolyzer used in HRES. This electrolyzer can produce about 2 [L] of hydrogen per minute. However, one electrolyzer cannot produce enough hydrogen. Therefore, 8 electrolyzers are used in this HRES. These eight electrolyzers were connected in parallel in four rows, as shown in Fig. 3-12, and the two were connected in series.

**Tab. 3-4 Electrolyzer's basic data [15]**


	Titan EZ-2000
	
Out put flow rate	0~2020 [ml/min]
Input volt	16 [V]
Input amp	0~36 [A]
Number of cells	8 [-]
Reaction area	50 [cm <sup>2</sup> ]

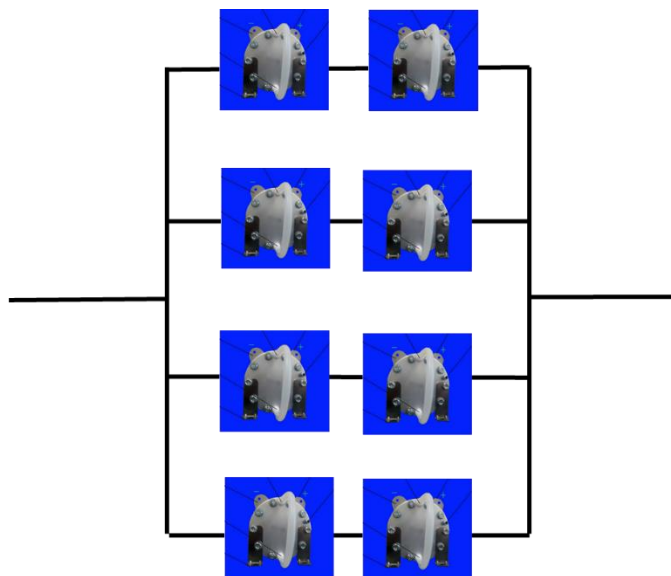


**Fig. 3-12 Electrolyzer connection diagram**

Tab. 3-5 shows the technical data of the fuel cell used for HRES. One Fuel cell can output about 1 [kW]. However, the power consumption may be over 1 [kW], as shown in Tab. 3-1. So, I will use two Fuel cells. In this case, it is possible to generate power up to 2 [kW] and cover all the power consumption shown in Fig. 3-13.

**Tab. 3-5 Basic data of fuel cell [20]**

	Horizon H-1000
	
A : Reaction area	72[ $cm^2$ ]
N : Number of cells	48[-]
<b>mH2</b> : Hydrogen flow rate	13 [L/min]
Lmen : Membrane thick ness	20[ $\mu m$ ]
<b>T</b> : Temperature	0~65 [°C]
$P_m$ : Maximum power output	1000 [W]
$I_m$ : Maximum power point current	35 [A]
$V_m$ : Maximum power point voltage	28.8 [V]

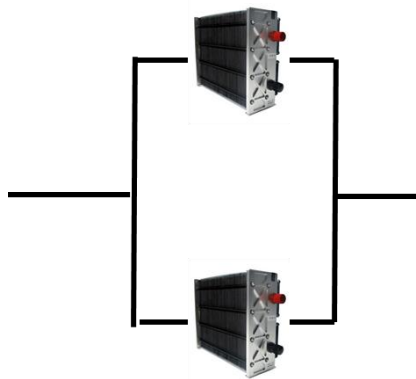


**Fig. 3-13 Fuel cell connection diagram**

## 4. Results and discussion

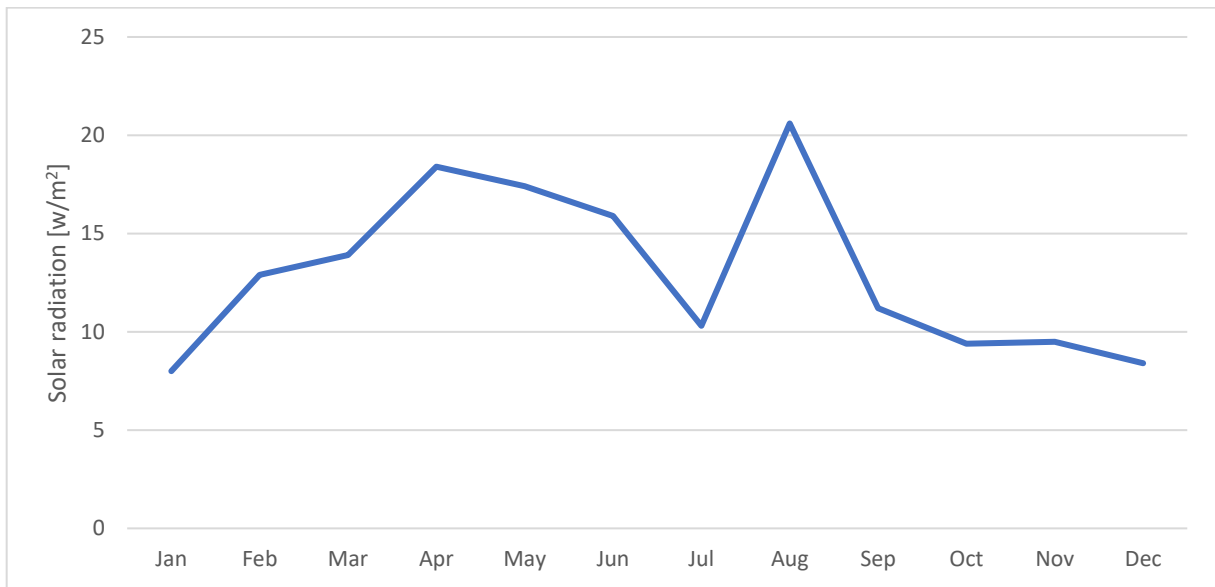
The proposed HRES is applied to the residential area in the city of Tokyo in Japan (Fig. 4-1).



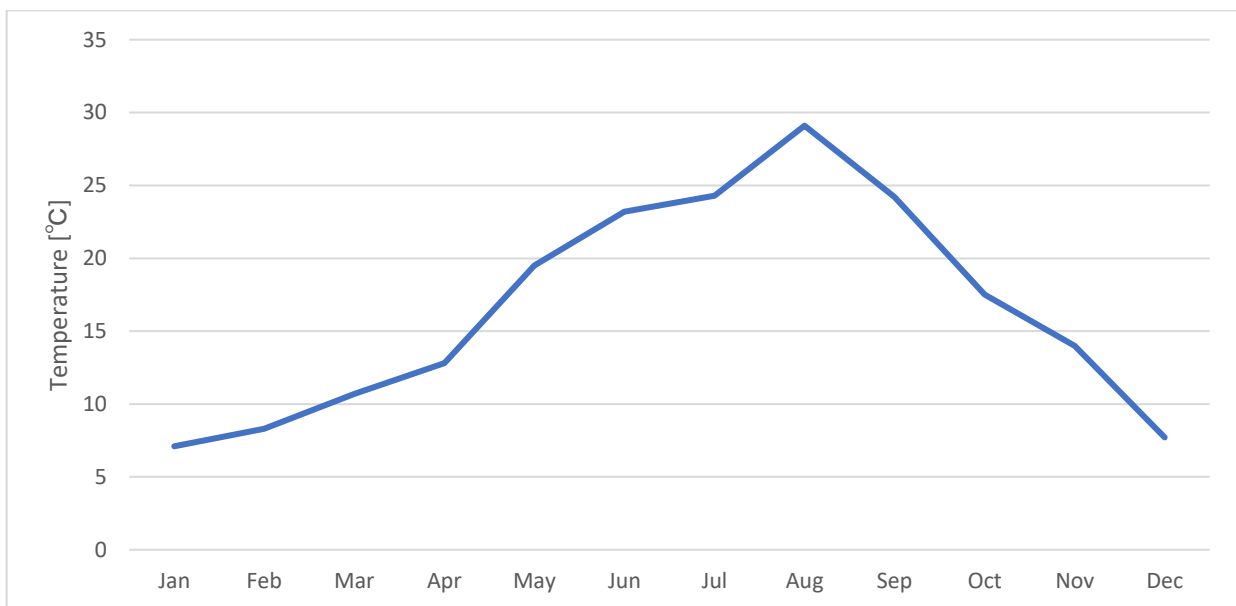
**Fig. 4-1 Tokyo map**

Fig. 4-2 shows the monthly average temperature in Tokyo. The amount of solar radiation is one of the most important parameters that greatly affect the output of the HRES. In July in Tokyo, the amount of solar radiation is weak. This seems to be due to the typhoon. The amount of solar radiation has weakened due to the typhoon.





**Fig. 4-2 Monthly solar radiation**



**Fig. 4-3 Monthly temperature**

One of the purposes of this research is to calculate the LCOE of each region. LCOE can be calculated from Eq (4-1).

$$\text{LCEO}[\text{Y/kWh}] = \frac{\text{Total cost [Y]}}{\text{Annual electricity generation[kWh]}} \quad (4-1)$$


The total cost of the HRES can be calculated as follows:

$$\text{Total Cost[Y]} = \text{Annualized cost of the HRES} + \text{operation cost of the HERS} \\ + \text{Purchasing electricity from the grid} - \text{Selling electricity to the grid} \quad (4-2)$$


In the above equation, the mismatch between electricity demand and the amount of electricity generated by the HREs should be purchased from the grid. The surplus solar electricity which cannot be used in the residential building will be sold back to the grid.

The total annualized cost consists of capital investment and operation and maintenance costs of the system. The cost of each element is described in Tab. 4-1 to Tab. 4-4.


**Tab. 4-1 PV panel's cost [6]**

	<b>VBHN330SJ47</b>
	
<b>Number of panels</b>	<b>28 [-]</b>
<b>Initial cost</b>	<b>198 [W] × 230 [yen/W] × 28[-] = 1275120[yen]</b>
<b>Life span</b>	<b>25 year</b>
<b>Maintenance cost</b>	<b>1275120 × 7% = 89258 yen</b>
<b>Total cost per year</b>	<b>88748 [yen/year] = <math>\frac{1275120 \text{ [yen]}}{25 \text{ [year]}} + \frac{89258 \text{ [yen]}}{25 \text{ [year]}}</math></b>


**Tab. 4-2 Electrolyzer's cost [15]**

	<b>Titan EZ-2000 Stack</b>
	
<b>Number of electrolyzer</b>	<b>8[-]</b>
<b>Initial cost</b>	<b>576[W] × 400 [W/yen] × 8[-] = 1843200[yen]</b>
<b>Life span</b>	<b>15 year</b>
<b>Maintenance cost</b>	<b>1843200 × 7% = 129024 yen</b>
<b>Total cost per year</b>	<b>128287 [yen/year] = <math>\frac{1843200 \text{ [yen]} \times 1.67[-]}{25 \text{ [year]}} + \frac{129024 \text{ [yen]}}{25 \text{ [year]}}</math></b>

Tab. 4-3 Fuel cell cost [20]

Horizon H-1000	
	
Number of fuel cell	2[-]
Initial cost	$1000[W] \times 400[W/yen] \times 2[-] = 80000[yen]$
Life span	9 [ year ]
Maintenance cost	$91200 \times 7\% = 56000 [ yen ]$
Total cost per year	$91200 [yen/year] = \frac{91200[yen] \times 2.78[-]}{25 [year]} + \frac{56000 [yen]}{25 [year]}$

Tab. 4-4 Hydrogen cost [21]

Hydrogen storage ( 7000L )	
	
Number of panel	1[-]
Initial cost	$22265[ \$ ] \times 120[yen/ \$ ] \times 1[-] = 267000[yen]$
Life span	15 year
Maintenance cost	$2671800 \times 7\% = 18690 [ yen ]$
Total cost per year	$18583 [yen/year] = \frac{267000 [yen] \times 1.67}{25[year]} + \frac{18690 [yen]}{25 [year]}$

Tab. 4-5 summarizes the annual cost of the HRES, which can be used in Eq. (4-1) .

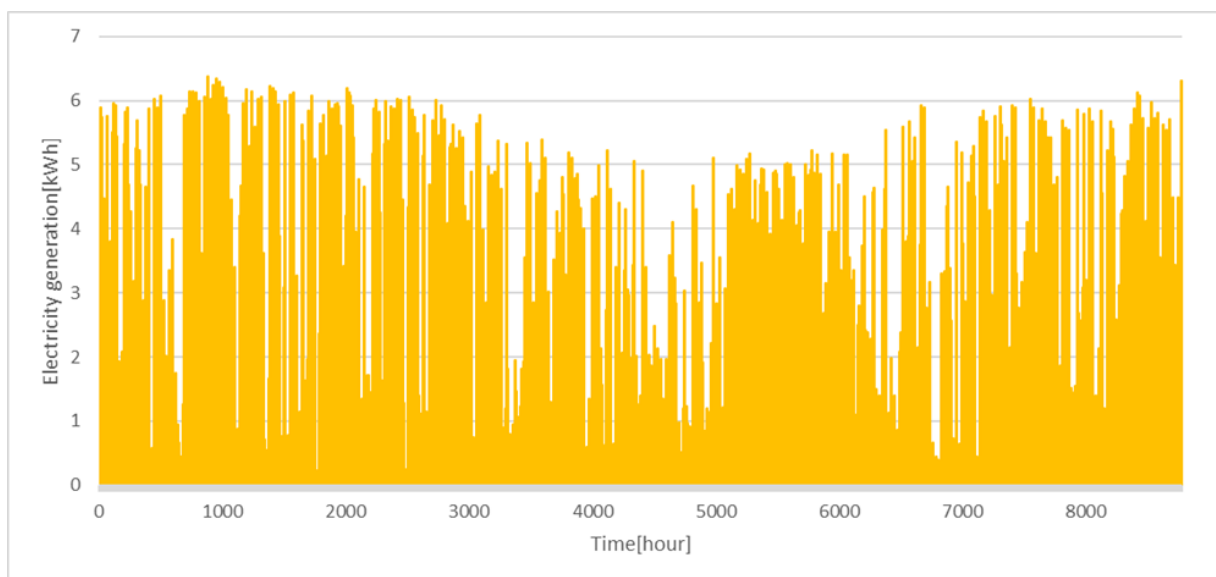
**Tab. 4-5 Annual cost of HRES**

<b>Each total</b>	
PVcost : PV cost [ yen/year ]	<b>88748</b>
FCcost ; Fuel cell [ yen/year ]	<b>128287</b>
ELcost : Electrolyzer [ yen/year ]	<b>91200</b>
H2Scost : Hydrogen storage cost [ yen/year ]	<b>18583</b>
HRES : HRES total cost [ yen/year ]	<b>326818</b>

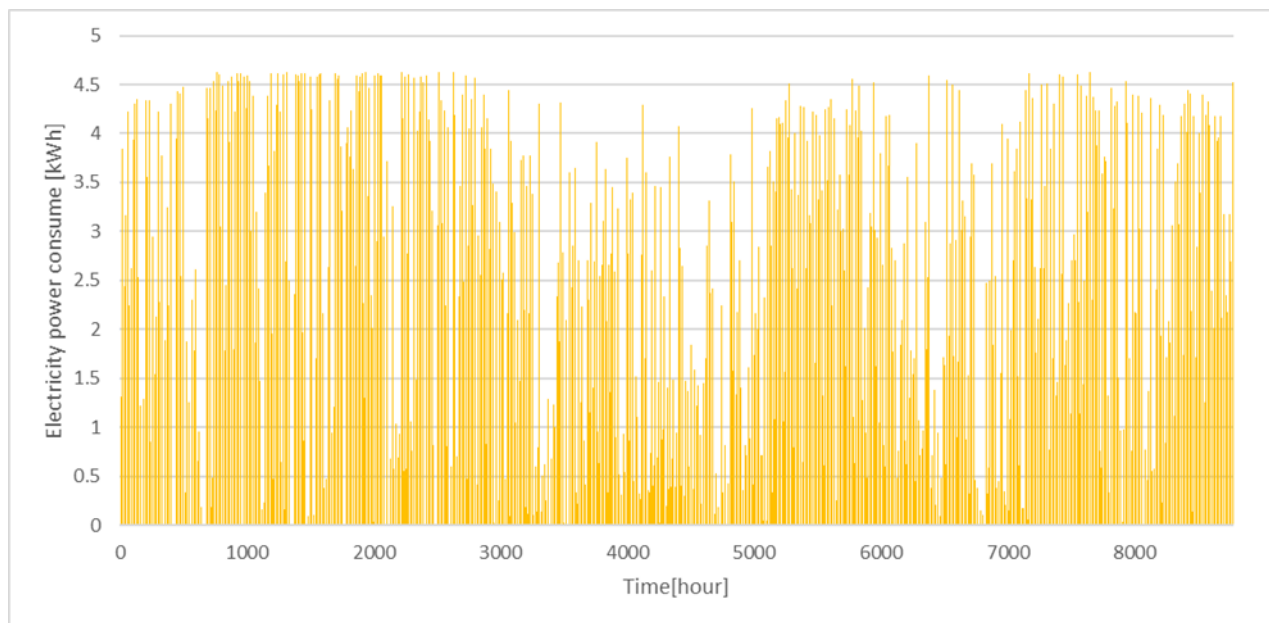
The Coverage ratio indicates the ratio of the generated electricity from the HRES to the total electricity demand of the residential building as follows;

$$\text{Coverage ratio [-]} = \frac{PV[kWh] + FC[kWh]}{\text{Demand}[kWh]} \quad (4-2)$$

Fig. 4-4 shows the amount of power generated by PV-panel per hour in Tokyo. Fig. 4-4 shows the output of the solar panel. Fig. 4-5 shows the electricity consumption in the electrolyzer. The input power of the electrolyzer is low during some summer periods due to reaching the maximum level in hydrogen storage.

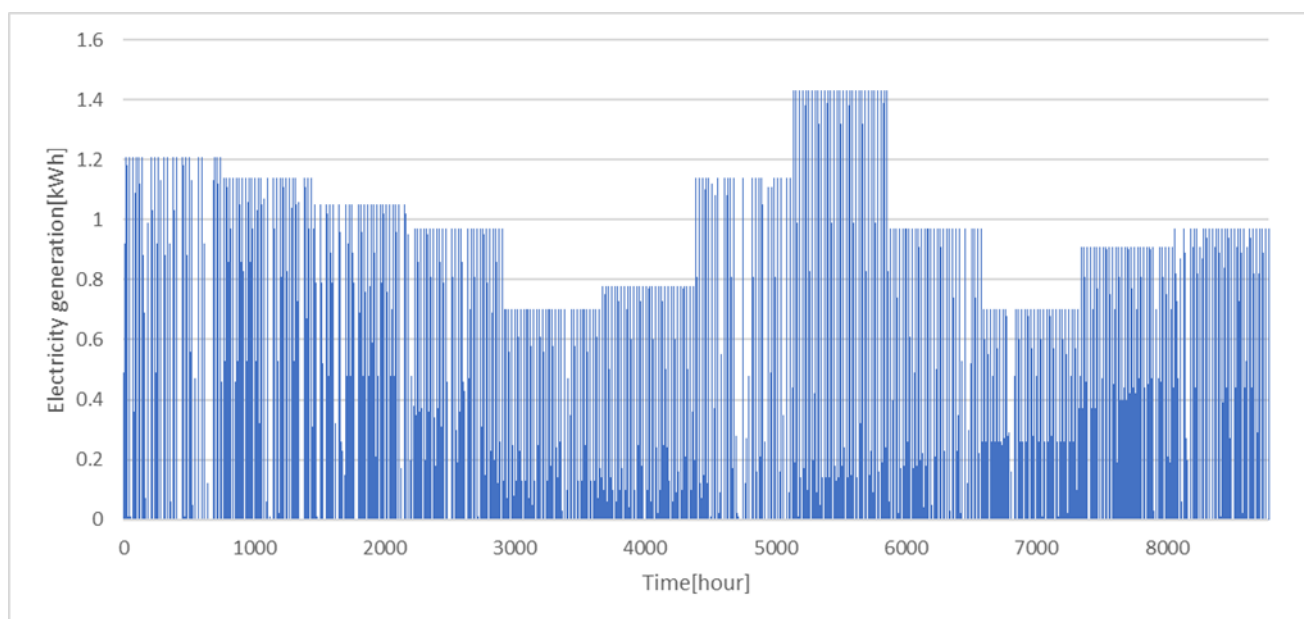


**Fig. 4-4 PV panel hourly electricity generation**



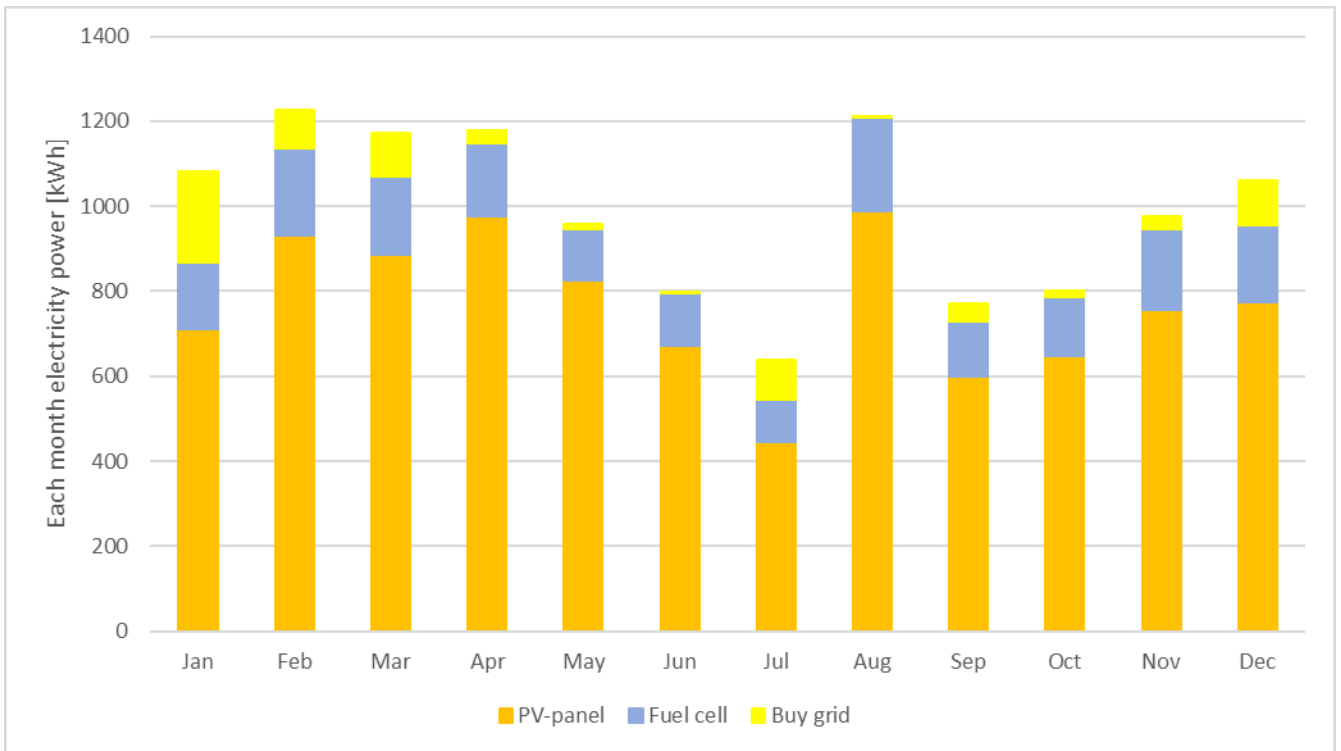
**Fig. 4-5 Electrolyzer hourly electricity consumption**

Fig. 4-6 shows the amount of electricity generated by the fuel cell per hour. Also, in July, the amount of solar radiation was low, and the electrolytic cell could not generate enough hydrogen, so the hydrogen storage became empty and the fuel cell stopped working at all for some time. This is also depicted in Fig. 4-7 and Fig. 4-8.



**Fig. 4-6 Fuel cell power output**

From Fig. 4-8, it can be observed that, the HERS boasts a high self-sufficiency rate of 90% or more from April to August. However, July has a low self-sufficiency rate of less than 90%. The amount of purchased electricity from the grid during the cold season is higher due to the lack of solar radiation and the availability of hydrogen. It can be seen that HRES can supply more than 90% of the electricity consumption from March to October. In addition, 87% or more of the power can be provided stably from HRES even at other times.



**Fig. 4-7 Monthly solar panel, fuel cell, grid power**

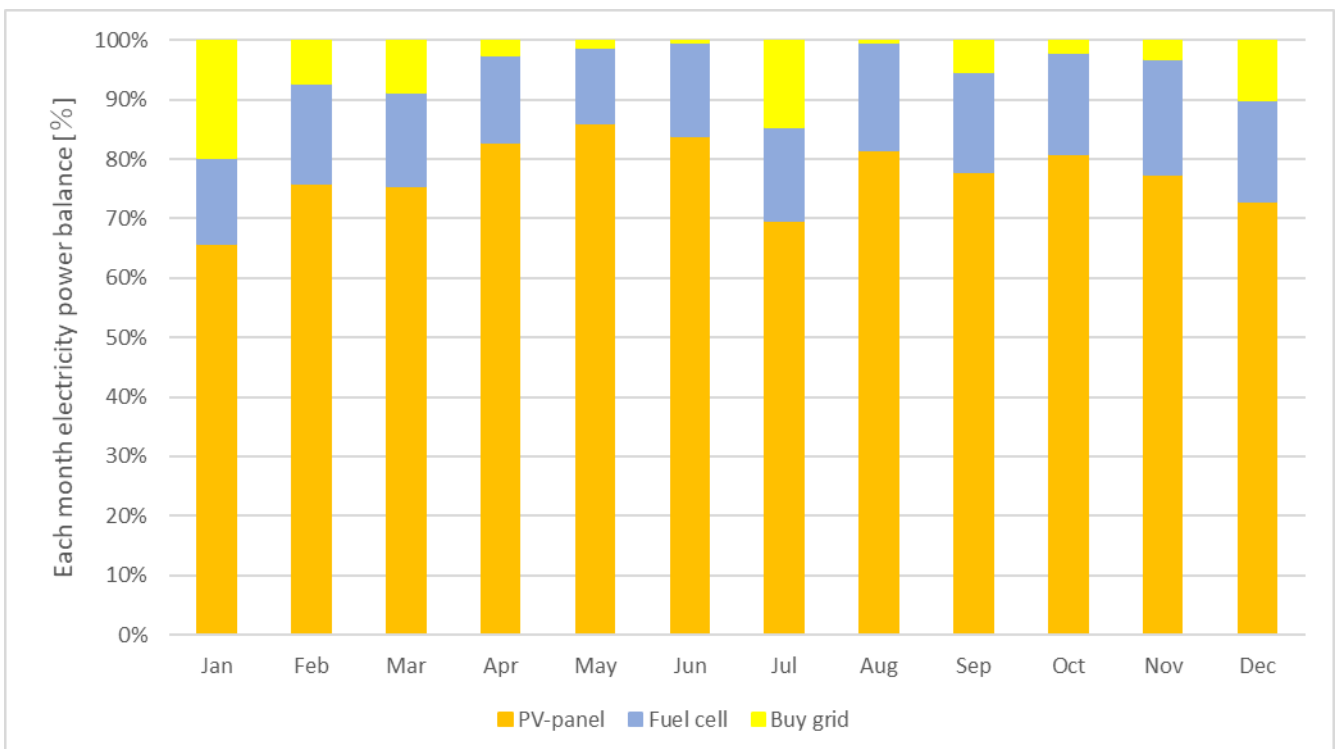


**Fig. 4-8 Monthly solar panel, fuel cell, grid power balance**

**Tab. 4-6 Annual electricity generation/consumption of the proposed HRES in Tokyo**

Each total	
PV consume [ kWh/year ]	1740
Fuel cell [ kWh/year ]	1925
Sell grid [ kWh/year ]	1336
Buy grid [ kWh/year ]	725
Demand [ kWh/year ]	4390
Coverage ratio [ - ]	0.835
LCOE [yen/kWh]	87

## 5- Conclusion

The main aim of this work in this thesis was to carry out a techno-economic analysis for a proposed HRES, which consists of PV modules, Fuel cell, and solar electrolyzer to be used in the residential areas in Tokyo, Japan. The calculation results are shown in Tab. 5-1.

**Tab. 5-1 Calculation results for Tokyo**

	Tokyo
Demand [kWh/year]	4390
Generation [kWh/year]	3665
From PV [kWh/year]	1740
From Fuel cell [kWh/year]	1925
Sell to grid [kWh/year]	1336
Buy from Grid [kWh/year]	725
Coverage ratio [-]	0.835
LCOE [yen/kWh]	87

By applying the proposed HRES in Tokyo residential area, about 83.5% of the total electricity demand requirement can be covered. Considering both the total capital cost investment and electricity generation, the LCO is estimated at 87 [yen/ kWh], which is about three times the current electricity tariff in Tokyo. The main reason for such high LCOE is the capital cost of the fuel cells, electrolytic cells, and hydrogen tank. The highest demand for solar hydrogen has resulted in increasing the share of the PV panels. By increasing the amount of hydrogen produced by the electrolyzer, the total cost of the system increases. Therefore, the reduction of the cost of the solar-hydrogen system turns out to be by far the most critical cost driver. Since, the fuel cell generates a considerable amount of exhaust gas with high temperature during the operation, this amount of waste heat can be recovered in a heat exchanger to provide sufficient hot water for the residential area and reduce the LCOE of the system.



## Reference

- 1 [Historic Total World Carbon Emissions Chart - a photo on Flickrriver](#)
- 2 <https://www.enecho.meti.go.jp/about/pamphlet/energy2018/html/001/>
- 3 <http://www.data.jma.go.jp/gmd/risk/obsdl/index.php>
- 4 Takatsu N., Farzaneh, H. (2020). Techno-Economic Analysis of a Novel Hydrogen-Based Hybrid Renewable Energy System for Both Grid-Tied and Off-Grid Power Supply in Japan: The Case of Fukushima Prefecture, *Applied Sciences*, 10(12), 4061
- 5 <https://www.youtube.com/watch?v=7Ryk3CD6EoM&feature=youtu.be>
- 6 Panasonic, “hit-325-w-PEM-power-panel catalog”
- 7 Hauck, B., Wang, W., & Xue, Y. (2021). On the model granularity and temporal resolution of residential PV battery system simulation. *Developments in the Built Environment*, 6, 100046. <https://doi.org/10.1016/j.dibe.2021.100046>
8. Zaimi, M., Achouby, H. E., Ibral, A., Assaid, E. M., & El Maliki, M. S. (2019). New analytical models for cardinal points of photovoltaic solar module operating outdoor under arbitrary conditions. 2019 7th International Renewable and Sustainable Energy Conference (IRSEC). <https://doi.org/10.1109/irsec48032.2019.9078298>
- 9 Tijani, A. S., & Rahim, A. A. (2016). Numerical modeling the effect of operating variables on Faraday efficiency in PEM Electrolyzer. *Procedia Technology*, 26, 419-427. <https://doi.org/10.1016/j.protcy.2016.08.054>
- 10 Scheepers, F., Stähler, M., Stähler, A., Rauls, E., Müller, M., Carmo, M., & Lehnert, W. (2021). Temperature optimization for improving polymer electrolyte membrane-water electrolysis system efficiency. *Applied Energy*, 283, 116270. <https://doi.org/10.1016/j.apenergy.2020.116270>
- 11 Escobar-Yonoff, R., Maestre-Cambronel, D., Charry, S., Rincón-Montenegro, A., & Portnoy, I. (2021). Performance assessment and economic perspectives of integrated PEM fuel cell and PEM electrolyzer for electric power generation. *Heliyon*, 7(3), e06506. <https://doi.org/10.1016/j.heliyon.2021.e06506>
- 12 Tijani, A. S., Binti Kamarudin, N. A., & Binti Mazlan, F. A. (2018). Investigation of the effect of charge transfer coefficient (CTC) on the operating voltage of polymer electrolyte membrane (PEM) electrolyzer. *International Journal of Hydrogen Energy*, 43(19), 9119-9132. <https://doi.org/10.1016/j.ijhydene.2018.03.111>
- 13 Tijani, A. S., Ghani, M. A., Rahim, A. A., Muritala, I. K., & Binti Mazlan, F. A. (2019). Electrochemical characteristics of (PEM) electrolyzer under influence of charge transfer coefficient. *International Journal of Hydrogen Energy*, 44(50), 27177-27189. <https://doi.org/10.1016/j.ijhydene.2019.08.188>
14. Titan, “series-technical-data-sheet”
15. Titan, “ez-2000-stack-manual”
16. Li, C., Ji, X., Zeng, Q., Wang, Y., & Wu, X. (2013). Modeling and performance analysis of a PEM fuel cell system. *Lecture Notes in Electrical Engineering*, 943-951. [https://doi.org/10.1007/978-1-4614-4981-2\\_102](https://doi.org/10.1007/978-1-4614-4981-2_102)
17. SALEH, I. M., ALI, R., & ZHANG, H. (2016). Simplified mathematical model of proton exchange membrane fuel cell based on horizon fuel cell stack. *Journal of Modern Power Systems and Clean Energy*, 4(4), 668-679. <https://doi.org/10.1007/s40565-016-0196-5>
18. Mann, R. F., Amphlett, J. C., Hooper, M. A., Jensen, H. M., Peppley, B. A., & Roberge, P. R. (2000). Development and application of a generalised steady-state electrochemical model for a PEM fuel cell. *Journal of Power Sources*, 86(1-2), 173-180. [https://doi.org/10.1016/s0378-7753\(99\)00484-x](https://doi.org/10.1016/s0378-7753(99)00484-x)
19. Horizon, ”H-30 Fuel Cell Stack”
20. Horizon, ”H-1000 Fuel Cell Stack”
21. MyH2® 7000